



5-2000

## **Verification of beam on elastic foundation solution for edge loaded cylindrical shells**

Sherry L. Caperton

Follow this and additional works at: [https://trace.tennessee.edu/utk\\_gradthes](https://trace.tennessee.edu/utk_gradthes)

---

### **Recommended Citation**

Caperton, Sherry L., "Verification of beam on elastic foundation solution for edge loaded cylindrical shells." Master's Thesis, University of Tennessee, 2000.  
[https://trace.tennessee.edu/utk\\_gradthes/9292](https://trace.tennessee.edu/utk_gradthes/9292)

This Thesis is brought to you for free and open access by the Graduate School at TRACE: Tennessee Research and Creative Exchange. It has been accepted for inclusion in Masters Theses by an authorized administrator of TRACE: Tennessee Research and Creative Exchange. For more information, please contact [trace@utk.edu](mailto:trace@utk.edu).

To the Graduate Council:

I am submitting herewith a thesis written by Sherry L. Caperton entitled "Verification of beam on elastic foundation solution for edge loaded cylindrical shells." I have examined the final electronic copy of this thesis for form and content and recommend that it be accepted in partial fulfillment of the requirements for the degree of Master of Science, with a major in Mechanical Engineering.

Remi Engels, Major Professor

We have read this thesis and recommend its acceptance:

Louis R. Decker

Accepted for the Council:

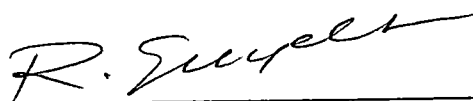
Carolyn R. Hodges

Vice Provost and Dean of the Graduate School

(Original signatures are on file with official student records.)

To the Graduate Council

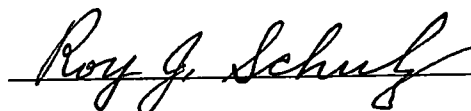
I am submitting herewith a dissertation written by Sherry L. Caperton entitled "Verification of Beam on Elastic Foundation Solution for Edge Loaded Cylindrical Shells." I have examined the final copy of this dissertation for form and content and recommend that it be accepted in partial fulfillment of the requirements for the degree of Master of Science, with a major in Mechanical Engineering



---

Remi Engels, Major Professor

We have read this dissertation  
and recommend its acceptance



---

Accepted for the Council



---

Associate Vice Chancellor and  
Dean of the Graduate School

VERIFICATION OF  
BEAM ON ELASTIC FOUNDATION SOLUTION  
FOR EDGE LOADED CYLINDRICAL SHELLS

A Thesis  
Presented for the  
Master of Science  
Degree  
The University of Tennessee, Knoxville

Sherry L Caperton  
May 2000

## ABSTRACT

The purpose of this thesis is to determine the range of radius to thickness ratios  $R/t$  for which a beam on an elastic foundation solution is feasible for end loadings on cylindrical shells. Using the finite element method a Saint-Venant's length, as defined in Chapter 1, is determined for several cylindrical geometries by loading one end of each cylinder with a shear load in six different ways. The standard deviation of the stress values is then computed to determine the distance from the load the stresses from each loading converge along the length of the cylinder on the inner and outer radii. A Saint-Venant's length is also determined in the same manner for the same cylindrical geometries for an end moment loading. The Saint-Venant's length for a cylinder geometry is then taken to be the more conservative of the two lengths. Taking this Saint-Venant's length into account the maximum circumferential or longitudinal stress is found and a percent error is computed between the results of a finite element solution and the analytical model based on a beam on an elastic foundation solution. This procedure is repeated for each cylinder geometry for both the end shear and end moment loads.

When the Saint-Venant's length is plotted against the ratio  $R/t$  for each cylinder geometry it is shown that the influence of the Saint-Venant's length decreases as cylinder walls get thinner. This allows the maximum stress to be taken closer to the end of the cylinder where the load is applied. The percent error between the finite element solution and the beam on an elastic foundation

solution is plotted against the ratio  $R/t$  for each cylindrical geometry allowing a range of ratios  $R/t$  to be determined for a given percent error. In this way, it can be determined whether or not a beam on an elastic foundation solution is satisfactory for a given geometry and required percent error.

## TABLE OF CONTENTS

CHAPTER	PAGE
I INTRODUCTION . . . . .	1
Purpose .. . . .	1
Scope .. . . .	1
II BEAM ON AN ELASTIC FOUNDATION . . . . .	4
Description of method. .. . . .	4
Equations . . . . .	7
Solutions using thick cylinder corrections ..	33
Classification of beams ... . . . .	36
III FINITE ELEMENT ANALYSIS . . . . .	39
Description of method . . . . .	39
Element type and mesh density. . . . .	39
Loading and boundary conditions ... . . . .	41
Other specifics used in the analysis. . . . .	44
Saint-Venant's length .. . . .	44
IV COMPARISON OF DATA ... . . . .	47
Comparison of results with experimental data.. ... . .	47
Comparison of analysis techniques for 15 0" and 7 5" cylinders . .	47
V CONCLUSIONS ... ..	59
Experimental data. . . . .	59
Saint-Venant's length .. . . .	60
Error.. . . .	60
Benefits .. . . .	62
Summary .. . . .	62
REFERENCES. . . . .	64
VITA .. . . .	67

## LIST OF FIGURES

FIGURE	PAGE
1 Load configurations for thick and thin cylindrical shells. . . .	2
2 Longitudinal beam element . . . . .	6
3 Shear loading on the end of a beam.. . . .	8
4 Moment loading on the end of a beam . . . . .	8
5 Forces exerted on a differential element from a beam on an elastic foundation .. . . .	9
6 An infinite beam subjected to a single concentrated force at point $O$ ...	13
7 An infinite beam with a single concentrated moment loading at point $O$ . . . . .	17
8 An infinite beam shown divided into symmetric and antisymmetric parts.. . . .	20
9. An infinite beam shown with end-conditioning forces . . . . .	22
10. A sector removed from a cylinder that is to be analyzed using beam on elastic foundation . . . . .	34
11. Axisymmetric elements and coordinate system. . . . .	40
12 Load cases for shear loading, $P$ , for 15.0" and 7.5" cylinders	42
13. Load cases for moment loading, $M$ , for 15.0" and 7.5" cylinders	43
14 Stress divided by load vs distance from load for moment load on 15.0" OD, 11.0" ID, 15.0" long cylinder.....	45
15. Stress divided by load vs distance from load for shear load on 15.0" OD, 10.0" ID, 15.0" long cylinder.... . . . .	48
16 Stress divided by load vs distance from load for shear load on 15.0" OD, 10.0" ID, 7.5" long cylinder. . . . .	49
17. Stress divided by load vs distance from load for moment load on 15.0" OD, 10.0" ID, 15.0" long cylinder .. . . .	50



18.	Stress divided by load vs distance from load for moment load on 15.0" OD, 10.0" ID, 7.5" long cylinder. . . . .	51
19.	Saint-Venant's length divided by length of cylinder vs radius to thickness (R/t) ratio for 15.0" cylinders . . . . .	53
20.	Saint-Venant's length divided by length of cylinder vs radius to thickness (R/t) ratio for 7.5" cylinders . . . . .	54
21.	Percent error vs. radius to thickness ratio between finite element results and beam on elastic foundation results for shear load on 15.0" cylinders... . . . .	55
22.	Percent error vs radius to thickness ratio between finite element results and beam on elastic foundation results for shear load on 7.5" cylinders . . . . .	56
23.	Percent error vs. radius to thickness ratio between finite element results and beam on elastic foundation results for moment load on 15.0" cylinders.... . . . .	57
24.	Percent error vs radius to thickness ratio between finite element results and beam on elastic foundation results for moment load on 7.5" cylinders . . . . .	58

## NOMENCLATURE

$a$	Denotes distance between two shear loads, in
$c$	$R - R_m$ , in
$E$	Modulus of Elasticity, psi
$I$	Moment of Inertia, in <sup>4</sup> /in
$k$	Beam modulus, lb/ in <sup>3</sup>
$l$	Length, in
$m$	Root of exponential equation
$M$	Moment, lb-in/in
$M_o, M_1$	Moment load, lb-in/in
$N$	Compressive hoop force, lb/in
$n$	Number of data points
$P, P_1$	Shear load, lb/in
$P$	Radial force on a longitudinal beam element, lb/in-in
$p$	Intensity, psi
$q$	Distributed loading on a beam, lb/in
$Q$	Shear, lb/in
$R$	Radius, in
$R_i$	Inside radius of cylinder, in
$R_m$	Mean radius of cylinder, in
$R_o$	Outside radius of cylinder, in

$t$	Thickness, in
$x$	Distance from end of beam to point of interest, in
$\bar{x}$	Arithmetic mean
$x'$	$l - x$ , in
$x_i$	Data point when finding $\bar{x}$
$X$	Denotes circumferential axis on longitudinal beam element of cylinder
$y$	Deflection, in
$Y$	Denotes radial axis on longitudinal beam element of cylinder
$Z$	Denotes longitudinal axis on longitudinal beam element of cylinder
$\varphi$	Sector angle, degrees
$\lambda$	Characteristic, $\text{in}^{-1}$
$\mu$	Poisson's ratio
$\theta$	Slope
$\sigma_L$	Longitudinal stress, psi
$\sigma_C$	Circumferential stress, psi

# CHAPTER 1

## INTRODUCTION

### **Purpose.**

This thesis deals with the problem of edge loading of cylindrical shells. For certain radius to thickness ratios  $R/t$ , the shell can be modeled as a beam on an elastic foundation. The problem can then be solved analytically without significant loss of accuracy.

The purpose of this thesis is to determine the range of ratios  $R/t$  for which a beam on an elastic foundation solution is acceptable. This is done by comparing beam on elastic foundation solutions for selected cylindrical shells to their corresponding solutions obtained by the finite element method, using the finite element method as a near exact solution. In this application the ratio  $R/t$  is defined as the mean radius  $R$  divided by the wall thickness  $t$  of the cylinder.

### **Scope.**

In Dohrmann's and Ives' paper, 'Experimental Investigation of Edge Loading of Thick Cylindrical Shells' [1], an epoxy-plastic cylinder, 10.0" ID, 15.0" OD and 15.0" long, was mechanically loaded with two different end loadings and strain measurements were taken on each cylinder. The first load case consisted of an inward shear load on the top end of the cylinder while the second was an inward moment load on the top end of the cylinder. Both load configurations are shown in Figure 1. The cylinder was then cut to 7.5" long and the procedure

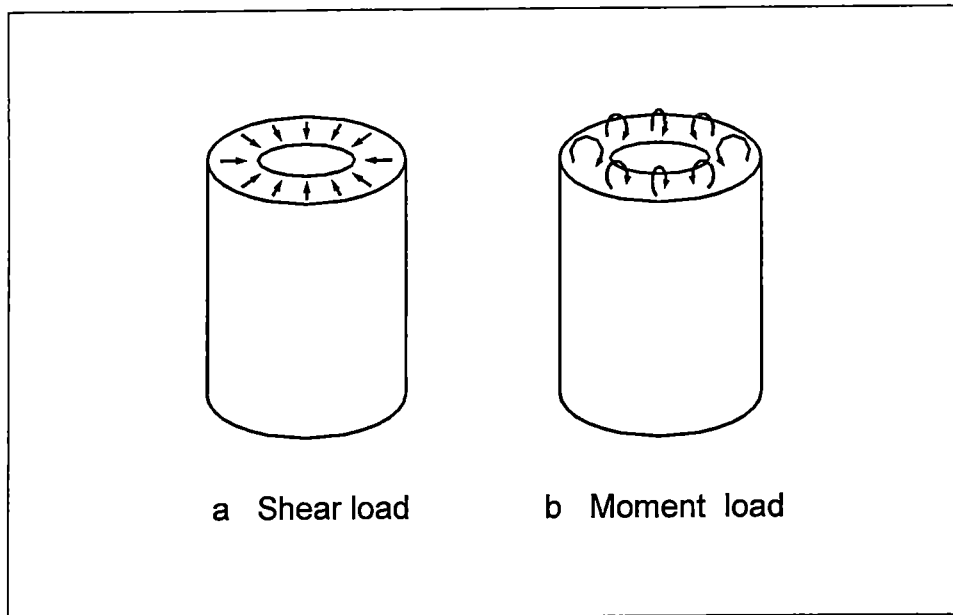


**Figure 1.** Load configurations for thick and thin cylindrical shells.

was repeated using the same loads. The longitudinal and circumferential stresses were examined for these cylinder geometries.

A finite element analysis and a beam on an elastic foundation analysis were performed by the author of the present study using the same cylinder geometries and types of loading as were used in Dohrmann's and Ives' experiment. The epoxy-plastic cylinder had a measured Modulus of Elasticity ( $E$ ) of 500,000 psi and a Poisson's Ratio ( $\mu$ ) of 0.375 [1]. The experimental data [1] is shown in Chapter 4 compared with the corresponding finite element and beam on elastic foundation data. Data was also obtained and compared for several other cylinder geometries using both analysis techniques in the present study. The percent error between the finite element results and the beam on an elastic foundation results for the longitudinal and circumferential stresses as

related to the ratio  $R/t$  are presented in Chapter 4 and discussed in Chapter 5. This data will be used to determine an  $R/t$  ratio interval for which the analytical beam on an elastic foundation solution can be readily used satisfactorily

The finite element data was also used to determine a Saint-Venant's length for each cylinder geometry. The principle of Saint-Venant is defined as follows.

“ . if the forces acting on a small portion of the surface of an elastic body are replaced by another statically equivalent system of forces acting on the same portion of the surface, this redistribution of loading produces substantial changes in the stresses locally but has a negligible effect on the stresses at distances which are large in comparison with the linear dimensions of the surface on which the forces are changed ” [2]

The Saint-Venant's length is defined as the distance away from the load where the method of loading no longer substantially effects the stresses. This Saint-Venant's length is taken into account in the comparison of the two analysis techniques. The influence of the Saint-Venant's length in relation to the ratio  $R/t$  is also presented and discussed in Chapters 4 and 5

## CHAPTER 2

### BEAM ON AN ELASTIC FOUNDATION

#### Description of method.

The first analysis technique applied to the loaded cylinders was that of a beam on an elastic foundation. A straight beam is supported continuously along its length by the 'foundation' which is considered to be elastic. For a beam on an elastic foundation analysis the 'foundation' is provided by a load-bearing medium distributed continuously along the length of the beam. When the beam is loaded and deflects, continuously distributed reaction forces appear in the foundation.

The fundamental assumption of a beam on an elastic foundation analysis is that at any point, the intensity,  $p$ , of these reaction forces is proportional to the deflection of the beam,  $y$ , at that point. Therefore,

$$p = ky \tag{1}$$

where  $k$  is the proportionality factor. The reaction forces act vertically in the foundation and oppose the deflection of the beam. Downward deflection is assumed to be positive causing compression in the foundation while upward deflection is negative causing tension [3].

There are two basic types of elastic foundations. For the first type, the pressure in the foundation is proportional at every point to the deflection in the beam at that point and is independent of other pressures or deflections

elsewhere in the foundation. This independence between pressures and deflections suggests a lack of continuity in the foundation, "just as if it were made up of rows of closely spaced but independent elastic springs" [4]. The second type of elastic foundation is an elastic solid which represents the case of complete continuity in the foundation. Most common problems can be reduced to elastic supporting conditions of the first type. Therefore, the problem dealt with in this thesis assumes a supporting medium of the discontinuous type [4].

The beam on an elastic foundation method may also be adapted for use with cylindrical bodies [5]. For cylindrical bodies under axially symmetrical loading the elastic foundation is supplied by the support of the adjacent sections of a continuous elastic structure. Because of the symmetry of the loading, every cross section perpendicular to the axis of the cylinder will remain circular while the radius  $R$  will experience a change. This change,  $\Delta R = y$ , will be different for each cross section along the length of the cylinder and may be regarded as a deflection for a longitudinal element which has a width of unity as seen in Figure 2. The loading will produce bending stresses in the longitudinal element. The strain  $y/R$  which accompanies the radial displacement  $y$  will cause compressive hoop forces  $N$  such that

$$N = \frac{Et}{R} y \quad (2)$$

per unit length of the longitudinal element, where  $E$  is the Modulus of Elasticity



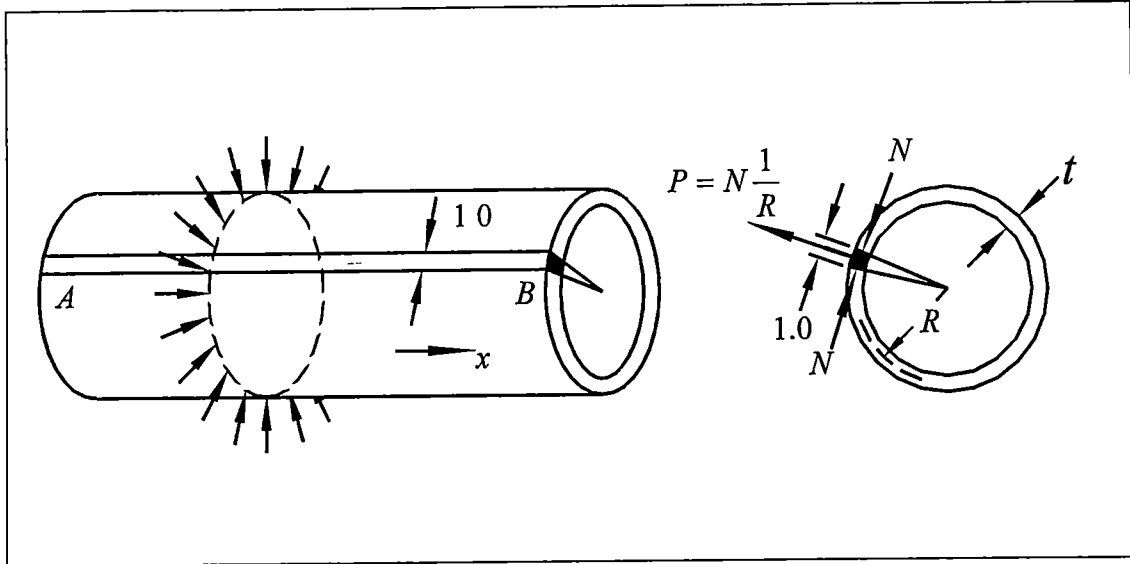


**Figure 2.** Longitudinal beam element A thin-walled cylindrical tube subjected to radial forces uniformly distributed along an arbitrary circle on the tube [5]

and  $t$  is the wall thickness. The resultant of these forces  $P$  will be in the outward radial direction and have the value

$$P = N \frac{1}{R} = \frac{Et}{R^2} y \quad (3)$$

This force  $P$  opposes the deflection and will also be proportional to the deflection with  $Et/R^2$  as the proportionality factor. Therefore, we may conclude that a longitudinal element of a cylindrical body loaded symmetrically with respect to its axis can be regarded as a beam on an elastic foundation.

A detailed account of this method can be found in Reference 3 and its thick cylinder adaptation can be found in Reference 6. MacGregor and Coffin [6] develop approximations of the beam on an elastic foundation equations to be

used with thick cylinders. However, for our purposes, Hetenyi's [7] equations for beams are used with the beam modulus  $k$  appropriate for cylinders as discussed in the next section (ref equations 111-114)

### **Equations.**

Equations may be derived for a number of different load cases. Hetenyi [14] suggests the method of superposition when deriving the beam on an elastic foundation equations because the determination of the integration constants is greatly simplified in comparison to other methods. The general procedure for this method begins by finding the equation for the deflection line of an infinitely long beam with a given loading. The formulas for the infinitely long beam are obtained in symmetrical and antisymmetrical parts and then superposed to obtain solutions for a beam of any length and with any loading and end conditions. Any frictional forces along the surface of the beam that is in contact with the foundation will be ignored since they are provided by second order equations. The load cases examined in this thesis are a shear loading on the end of a cylinder and a moment loading on the end of a cylinder, shown respectively in Figures 3 and 4 as applied to a beam on an elastic foundation. For these cases, the cylinder is assumed to have free ends.

Take an infinitely small element enclosed between two vertical cross sections from a part of a beam on an elastic foundation which is loaded by a distributed loading  $q$  [15]. These cross sections are a distance  $dx$  apart and it is assumed that the slope is negligible so that the cross sections,

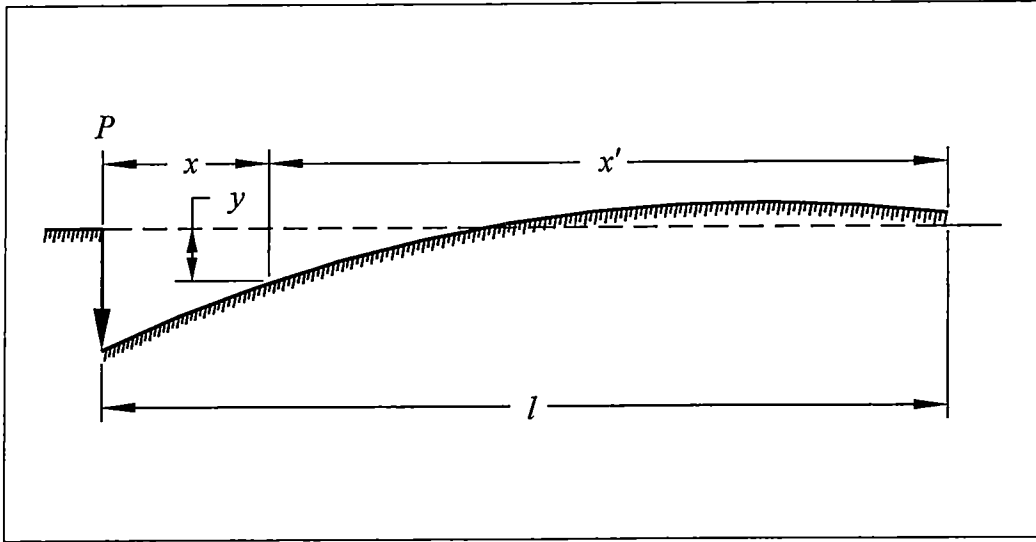


**Figure 3.** Shear loading on the end of a beam [7].

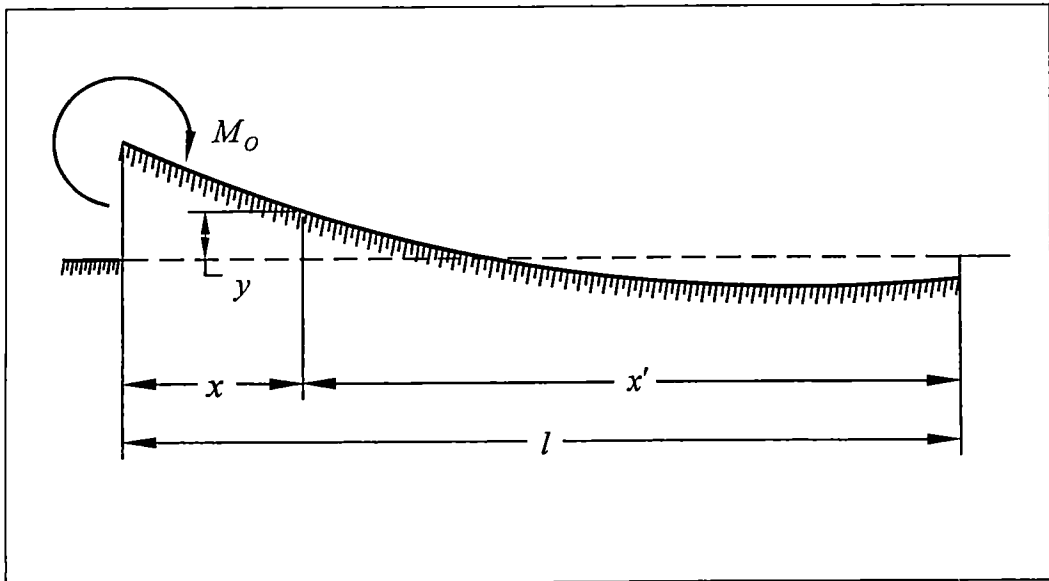


**Figure 4.** Moment loading on the end of a beam [7]

which are normal to the elastic line, can be replaced by vertical sections. The forces acting on this element and their positive directions are shown in Figure 5.

The shearing force  $Q$ , and the bending moment  $M$ , on the left side of the element are considered to be positive. Summing the forces on the element in the vertical direction gives

$$\frac{dQ}{dx} = ky - q. \quad (4)$$

Since

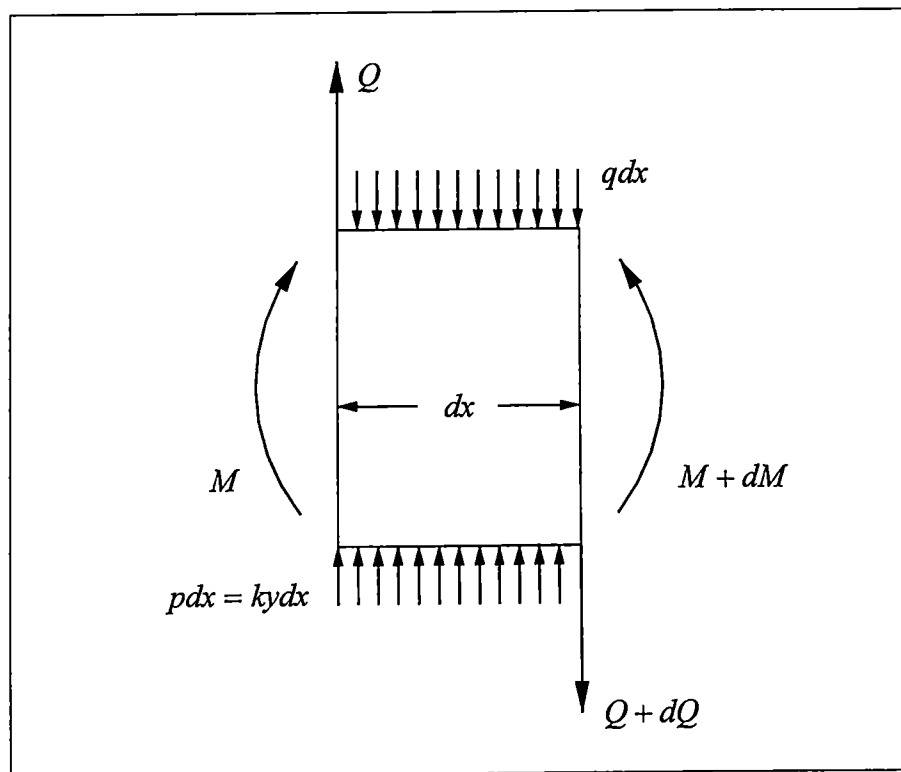


**Figure 5.** Forces exerted on a differential element from a beam on an elastic foundation [15]

$$Q = \frac{dM}{dx} \quad (5)$$

equation 4 can be rewritten as

$$\frac{dQ}{dx} = \frac{d^2M}{dx^2} = ky - q \quad (6)$$

The equation of fundamental beam theory [12] is

$$EI \frac{d^2y}{dx^2} = -M \quad (7)$$

Differentiating this equation twice and substituting into equation 6 gives

$$EI \frac{d^4y}{dx^4} = -ky + q \quad (8)$$

Equation 8 is the differential equation for the deflection curve of a beam supported on an elastic foundation. For portions of the beam where no distributed load is acting,  $q = 0$ , and the equation becomes

$$EI \frac{d^4y}{dx^4} = -ky \quad (9)$$

It is necessary to find the general solution of equation 9 For cases involving a distributed load an integral corresponding to  $q$  is added to this general solution

For the purposes of this thesis, a distributed loading is not explored.

Assuming a solution as

$$y = e^{mx} \quad (10)$$

and substituting into equation 9 gives

$$m^4 = -\frac{k}{EI} \quad (11)$$

Using De Moivre's Theorem [13], the roots of equation 11 are found to be

$$m_1 = -m_3 = \lambda(1 + i) \quad (12)$$

$$m_2 = -m_4 = \lambda(-1 + i) \quad (13)$$

where

$$\lambda = \sqrt[4]{\frac{k}{4EI}} \quad (14)$$

The general solution of the fundamental beam equation takes the form

$$y = A_1 e^{m_1 x} + A_2 e^{m_2 x} + A_3 e^{m_3 x} + A_4 e^{m_4 x} \quad (15)$$

where  $A_1$ ,  $A_2$ ,  $A_3$ , and  $A_4$  are unknown constants Using

$$e^{i\lambda x} = \cos \lambda x + i \sin \lambda x, \quad (16)$$

$$e^{-i\lambda x} = \cos \lambda x - i \sin \lambda x, \quad (17)$$

$$e^z = e^{x+iy} = e^x e^{iy} = e^x (\cos y + i \sin y), \quad (18)$$

and introducing new constants  $C_1$ ,  $C_2$ ,  $C_3$ , and  $C_4$  where

$$(A_1 + A_4) = C_1, \quad (19)$$

$$i(A_1 - A_4) = C_2, \quad (20)$$

$$(A_2 + A_3) = C_3, \quad (21)$$

$$i(A_2 - A_3) = C_4, \quad (22)$$

the general solution for the equation for the deflection curve for a beam on an elastic foundation can be written as

$$y = e^{\lambda x}(C_1 \cos \lambda x + C_2 \sin \lambda x) + e^{-\lambda x}(C_3 \cos \lambda x + C_4 \sin \lambda x) \quad [15] \quad (23)$$

For an infinite beam subjected to a single concentrated force at point  $O$  [16] as shown in Figure 6, symmetry allows consideration of  $x > 0$  while everything to the left of the load is ignored. Since the beam is infinite it is assumed that  $x \rightarrow \infty, y \rightarrow 0$ . For this to be true,  $C_1$  and  $C_2$  must be zero in equation 23. Therefore, the equation for the deflection curve for the part of the beam for which  $x > 0$  will be

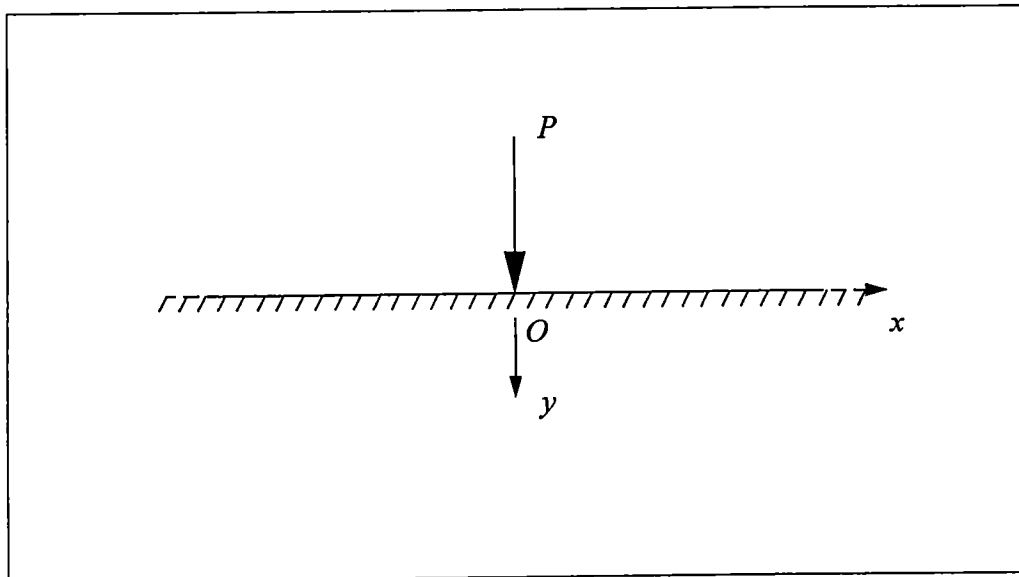


**Figure 6.** An infinite beam subjected to a single concentrated force at point  $O$  [16]



$$y = e^{-\lambda x} (C_3 \cos \lambda x + C_4 \sin \lambda x) \quad (24)$$

Because of symmetry, the slope at  $x = 0$  on the beam will be zero, or

$$\left[ \frac{dy}{dx} \right]_{x=0} = 0, \quad (25)$$

and, therefore,

$$C_3 = C_4 = C. \quad (26)$$

The equation for the deflection curve now becomes

$$y = Ce^{-\lambda x} (\cos \lambda x + \sin \lambda x). \quad (27)$$

The constant  $C$  is found by using the assumption that the sum of the reaction forces will be in equilibrium with the load  $P$ , or, as previously stated

$$P = ky. \quad (28)$$

Therefore, to find the load over the length of the beam the integration, making use of symmetry, is

$$2 \int_0^{\infty} ky dx = P. \quad (29)$$

Substituting equation 27 into equation 29,

$$2kC \int_0^{\infty} e^{-\lambda x} (\cos \lambda x + \sin \lambda x) dx = P \quad (30)$$

from which

$$C = \frac{P\lambda}{2k} \quad (31)$$

Substituting equation 31 into equation 27, the equation for the deflection curve for  $x \geq 0$  becomes

$$y = \frac{P\lambda}{2k} e^{-\lambda x} (\cos \lambda x + \sin \lambda x) \quad [16] \quad (32)$$

The slope  $\theta$ , moment  $M$ , and shear  $Q$ , can be found by taking successive derivatives of the equation for the deflection  $y$ . These formulas for  $x \geq 0$  are

$$\theta = -\frac{P\lambda^2}{k} e^{-\lambda x} \sin \lambda x \quad (33)$$

$$M = \frac{P}{4\lambda} e^{-\lambda x} (\cos \lambda x - \sin \lambda x) \quad (34)$$

$$Q = -\frac{P}{2} e^{-\lambda x} \cos \lambda x \quad [16] \quad (35)$$

To simplify the equations, the symbols

$$A_{\lambda x} = e^{-\lambda x} (\cos \lambda x + \sin \lambda x) \quad (36)$$

$$B_{\lambda x} = e^{-\lambda x} \sin \lambda x \quad (37)$$

$$C_{\lambda x} = e^{-\lambda x} (\cos \lambda x - \sin \lambda x) \quad (38)$$

$$D_{\lambda x} = e^{-\lambda x} (\cos \lambda x) \quad (39)$$

are substituted for  $y$ ,  $\theta$ ,  $M$ , and  $Q$  so that for a single concentrated force  $P$

$$y = \frac{P\lambda}{2k} A_{\lambda x} \quad (40)$$

$$\theta = -\frac{P\lambda^2}{k} B_{\lambda x} \quad (41)$$

$$M = \frac{P}{4\lambda} C_{\lambda x} \quad (42)$$

$$Q = -\frac{P}{2} D_{\lambda x} \quad [16] \quad (43)$$

Now it is necessary to examine the case for a single concentrated moment,  $M_0$ , applied at point  $O$  [16] as shown in Figure 7a. Figure 7b shows the moment force as it is represented by two point forces on each side of point  $O$ . The assumption is made that while  $a$  approaches zero ( $a \rightarrow 0$ ),  $P \times a$  will

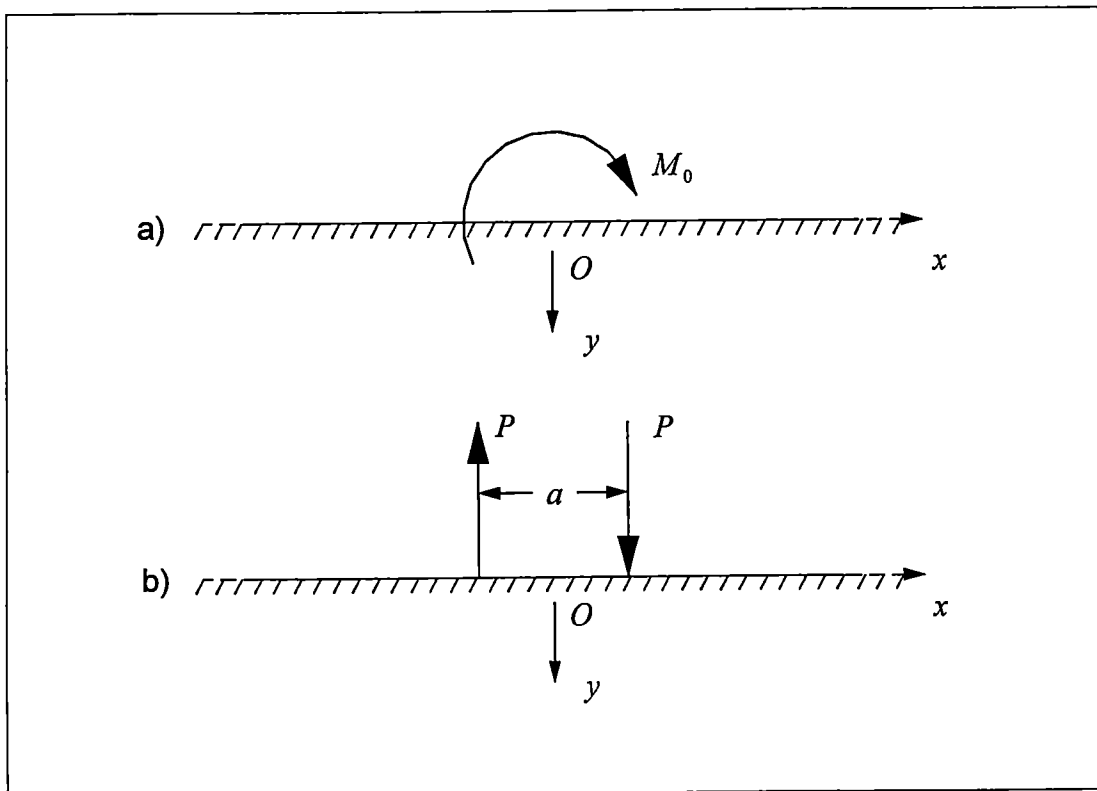


**Figure 7.** An infinite beam with a single concentrated moment loading at point  $O$  [16]

approach the value of  $M_0$  ( $P \times a \rightarrow M_0$ ) Using equation 40, the formula for the deflection curve for a single concentrated force  $P$ , the equation for the deflection line for the loading situation shown in Figure 7b for  $x \geq 0$  can be written as

$$y = \frac{P\lambda}{2k} (-A_{\lambda(x+a)} + A_{\lambda x}) = -\frac{Pa\lambda}{2k} \left( \frac{A_{\lambda(x+a)} - A_{\lambda x}}{a} \right) \quad (44)$$

Using the definition of a derivative [19] and the assumption that  $[P \times a]_{a \rightarrow 0} = M_0$ , it can be shown that

$$y = \frac{M_0 \lambda^2}{k} B_{\lambda x} \quad [16]. \quad (45)$$

This is the equation for the deflection line due to a clockwise moment  $M_0$  at point  $O$  as indicated in Figure 7a. As before with the single concentrated force, taking consecutive derivatives of the deflection  $y$  gives

$$\theta = \frac{M_0 \lambda^3}{k} C_{\lambda x} \quad (46)$$

$$M = \frac{M_0}{2} D_{\lambda x} \quad (47)$$

$$Q = -\frac{M_0 \lambda}{2} A_x \quad [16] \quad (48)$$

To obtain equations for a finite beam, the required loading is applied to an infinite beam and then resolved into a symmetrical and an antisymmetrical part. Forces which create the required conditions at the endpoints of the finite beam, called end-conditioning forces, are found for both parts. The purpose of these end-conditioning forces is to make the moments and shears vanish at the endpoints of the finite beam. The symmetrical and antisymmetrical parts are then added together at the endpoints to obtain the solution [17].

Consider the infinite beam shown in Figure 8a.  $M_A$ ,  $Q_A$ ,  $M_B$ , and  $Q_B$  are the moments and shears at points  $A$  and  $B$  due to the actual loading on the beam. In Figure 8b,  $M'_A$  and  $Q'_A$  are the moment and shear at  $A$  due to the symmetrical loading and  $M'_A$  and  $-Q'_A$  are the values at  $B$ . In Figure 8c,  $M''_A$  and  $Q''_A$  represent the moment and shear at  $A$  due to the antisymmetrical loading and  $-M''_A$  and  $Q''_A$  are the values at  $B$ . Since adding the symmetrical and the antisymmetrical parts together gives the end forces for the original given loading it follows that

$$M_A = M'_A + M''_A \quad (49)$$

$$M_B = M'_A - M''_A \quad (50)$$

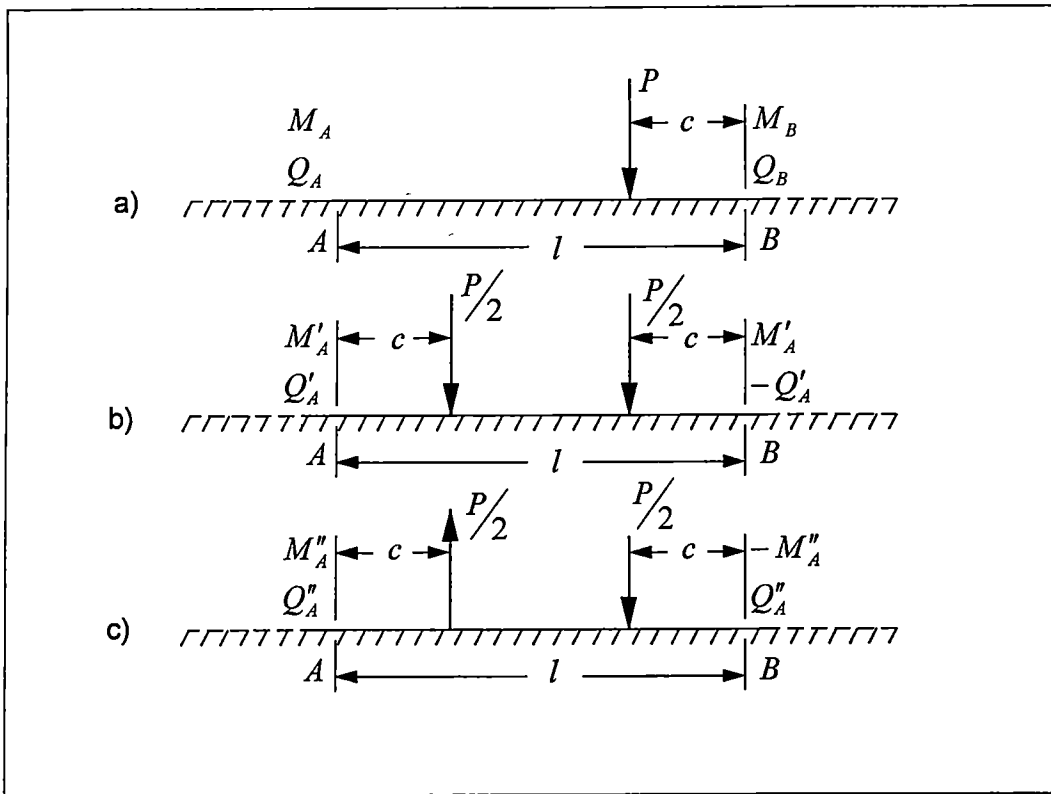


**Figure 8.** An infinite beam shown divided into symmetric and antisymmetric parts [17]

$$Q_A = Q'_A + Q''_A \quad (51)$$

$$Q_B = -Q'_A + Q''_A \quad (52)$$

Solving equations 49-52 for the separate symmetrical and antisymmetrical parts of the end forces

$$M'_A = \frac{1}{2}(M_A + M_B) \quad (53)$$

$$M_A'' = \frac{1}{2}(M_A - M_B) \quad (54)$$

$$Q_A' = \frac{1}{2}(Q_A - Q_B) \quad (55)$$

$$Q_A'' = \frac{1}{2}(Q_A + Q_B) \quad (56)$$

Next, the moment and shear forces at end points  $A$  and  $B$  will be removed by applying the end-conditioning forces  $P_0'$  and  $M_0'$  at these points in the symmetrical case and  $P_0''$  and  $M_0''$  for the antisymmetrical case as shown in Figure 9b-c. Adding the symmetrical and antisymmetrical cases together gives the end-conditioning forces for the infinite beam with the original loading shown in Figure 9a as

$$P_{0A} = P_0' + P_0'' \quad (57)$$

$$P_{0B} = P_0' - P_0'' \quad (58)$$

$$M_{0A} = M_0' + M_0'' \quad (59)$$

$$M_{0B} = M_0' - M_0'' \quad (60)$$



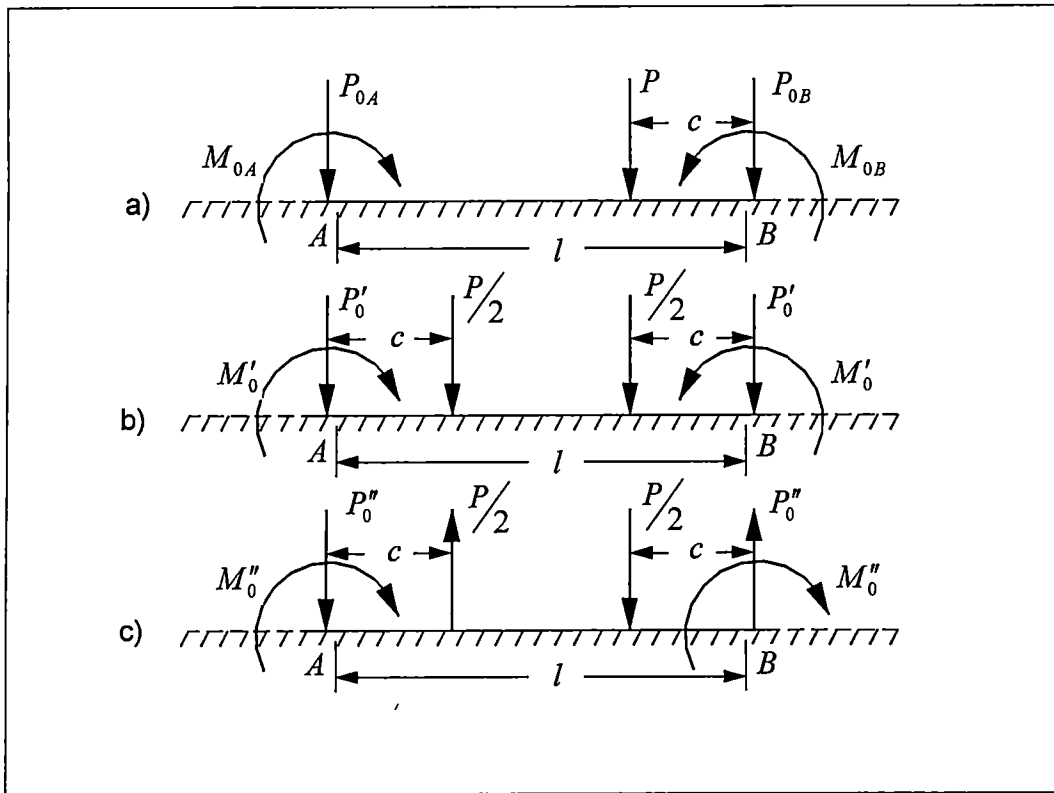


**Figure 9.** An infinite beam shown with end-conditioning forces [17].

These forces are required to remove the moments and shears at points  $A$  and  $B$ . This means that  $P_{0A}$ ,  $M_{0A}$ ,  $P_{0B}$ , and  $M_{0B}$  must produce  $-M_A$  and  $-Q_A$  at point  $A$  and  $-M_B$  and  $-Q_B$  at point  $B$ . It is seen from examination of Figures 8 and 9 that  $P'_0$  and  $M'_0$  must produce  $-M'_A$  and  $-Q'_A$  at point  $A$  and  $-M'_A$  and  $Q'_A$  at point  $B$  for the symmetrical beam. On the antisymmetrical beam,  $P''_0$  and  $M''_0$  must produce  $-M''_A$  and  $-Q''_A$  at point  $A$  and  $M''_A$  and  $-Q''_A$  at point  $B$ .

Using the conditions stated above and the moment and shear formulas for a single concentrated point force, equations 42 and 43, and a single

concentrated moment, equations 47 and 48, found earlier, the end-conditioning forces for the symmetrical and antisymmetrical parts of the beam are found to be

$$P'_0 = 4E_I [Q'_A(1 + D_{\lambda'}) + \lambda M'_A(1 - A_{\lambda'})] \quad (61)$$

$$M'_0 = -\frac{2}{\lambda} E_I [Q'_A(1 + C_{\lambda'}) + 2\lambda M'_A(1 - D_{\lambda'})] \quad (62)$$

$$P''_0 = 4E_{II} [Q''_A(1 - D_{\lambda'}) + \lambda M''_A(1 + A_{\lambda'})] \quad (63)$$

$$M''_0 = -\frac{2}{\lambda} E_{II} [Q''_A(1 - C_{\lambda'}) + 2\lambda M''_A(1 + D_{\lambda'})] \quad (64)$$

where  $E_I$  is

$$E_I = \frac{1}{2(1 + D_{\lambda'})(1 - D_{\lambda'}) - (1 - A_{\lambda'})(1 + C_{\lambda'})} \quad (65)$$

and  $E_{II}$  is

$$E_{II} = \frac{1}{2(1 + D_{\lambda'})(1 - D_{\lambda'}) - (1 + A_{\lambda'})(1 - C_{\lambda'})} \quad [17]. \quad (66)$$

These formulas will give the solution for a beam of finite length with free

ends subjected to any lateral loading since any value can be assigned to  $M_A$  and  $Q_A$ .

For the end shear load of interest for this thesis, the original loading will give  $M_A = 0$ ,  $Q_A = +P_1$ ,  $M_B = 0$ , and  $Q_B = 0$ . From this and from equations 53-56, the forces on the symmetrical and antisymmetrical portions of the beam will be

$$M'_A = 0 \quad (67)$$

$$Q'_A = \frac{P_1}{2} \quad (68)$$

$$M''_A = 0 \quad (69)$$

$$Q''_A = \frac{P_1}{2}. \quad (70)$$

The end-conditioning forces for the symmetrical part of the beam are then found from equations 61-64 to be

$$P'_0 = 4E_I \left[ \frac{P_1}{2} (1 + D_M) \right] \quad (71)$$

$$M'_0 = -\frac{2}{\lambda} E_I \left[ \frac{P_1}{2} (1 + C_{\lambda}) \right] \quad (72)$$

and for the antisymmetrical part of the beam

$$P''_0 = 4E_{II} \left[ \frac{P_1}{2} (1 - D_{\lambda}) \right] \quad (73)$$

$$M''_0 = -\frac{2}{\lambda} E_{II} \left[ \frac{P_1}{2} (1 - C_{\lambda}) \right] \quad (74)$$

Adding the symmetrical and antisymmetrical parts of the beam together as shown in equations 57-60 gives

$$P_{0A} = 2P_1 [E_I (1 + D_{\lambda}) + E_{II} (1 - D_{\lambda})] \quad (75)$$

$$P_{0B} = 2P_1 [E_I (1 + D_{\lambda}) - E_{II} (1 - D_{\lambda})] \quad (76)$$

$$M_{0A} = -\frac{P_1}{\lambda} [E_I (1 + C_{\lambda}) + E_{II} (1 - C_{\lambda})] \quad (77)$$

$$M_{0B} = -\frac{P_1}{\lambda} [E_I (1 + C_{\lambda}) - E_{II} (1 - C_{\lambda})] \quad (78)$$

Next, the deflection and moment must be found for each end-conditioning force since these are the quantities used to determine the stresses along the surface of the cylinder. The end-conditioning forces in equations 75-78 are substituted into the deflection and moment formulas for a single concentrated point force, equations 40 and 42, and a single concentrated moment, equations 45 and 47, found earlier. The deflections for the end-conditioning forces are

$$y(P_{0A}) = \frac{P_1 \lambda}{k} [E_I (1 + D_{\lambda}) + E_{II} (1 - D_{\lambda})] A_{\lambda x} \quad (79)$$

$$y(P_{0B}) = \frac{P_1 \lambda}{k} [E_I (1 + D_{\lambda}) - E_{II} (1 - D_{\lambda})] A_{\lambda x} \quad (80)$$

$$y(M_{0A}) = -\frac{P_1 \lambda}{k} [E_I (1 + C_{\lambda}) + E_{II} (1 - C_{\lambda})] B_{\lambda x} \quad (81)$$

$$y(M_{0B}) = -\frac{P_1 \lambda}{k} [E_I (1 + C_{\lambda}) - E_{II} (1 - C_{\lambda})] B_{\lambda x} \quad (82)$$

Adding the deflections in equations 79-82 together gives the deflection formula for a finite beam on an elastic foundation with free ends, loaded with a shear load on one end as

$$y = \frac{2P_1 \lambda}{k} E_I [(1 + D_{\lambda}) A_{\lambda x} - (1 + C_{\lambda}) B_{\lambda x}] \quad (83)$$

where  $P_1$  is the applied shear load.

The moments for the end-conditioning forces are found to be

$$M(P_{0A}) = \frac{P_1}{2\lambda} [E_I (1 + D_{\lambda}) + E_{II} (1 - C_{\lambda})] C_{\lambda x} \quad (84)$$

$$M(P_{0B}) = \frac{P_1}{2\lambda} [E_I (1 + D_{\lambda}) - E_{II} (1 - C_{\lambda})] C_{\lambda x} \quad (85)$$

$$M(M_{0A}) = -\frac{P_1}{2\lambda} [E_I (1 + C_{\lambda}) + E_{II} (1 - C_{\lambda})] D_{\lambda x} \quad (86)$$

$$M(M_{0B}) = -\frac{P_1}{2\lambda} [E_I (1 + C_{\lambda}) - E_{II} (1 - C_{\lambda})] D_{\lambda x} \quad (87)$$

Adding equations 84-87 together, the moment formula is

$$M = \frac{P_1}{\lambda} E_I [(1 + D_{\lambda}) C_{\lambda x} - (1 + C_{\lambda}) D_{\lambda x}] \quad (88)$$

For the moment load of interest in this thesis applied to the end of a cylinder,  $M_A = -M_1$ ,  $Q_A = 0$ ,  $M_B = 0$ , and  $Q_B = 0$ . From equations 53-56, the forces on the symmetrical and antisymmetrical portions of the beam will be

$$M'_A = -\frac{M_1}{2} \quad (89)$$

$$Q'_A = 0 \quad (90)$$

$$M''_A = -\frac{M_1}{2} \quad (91)$$

$$Q''_A = 0. \quad (92)$$

The end-conditioning forces for the symmetrical part of the beam can then be found from equations 61-64 to be

$$P'_0 = -2E_I \lambda [M_1(1 - A_{\lambda})] \quad (93)$$

$$M'_0 = 2E_I \left[ \frac{M_1}{2} (1 - D_{\lambda}) \right] \quad (94)$$

and for the antisymmetrical part of the beam

$$P''_0 = -2E_{II} \lambda [M_1(1 + A_{\lambda})] \quad (95)$$

$$M''_0 = 2E_{II} [M_1(1 + D_{\lambda})]. \quad (96)$$

Adding the symmetrical and antisymmetrical parts of the beam together as shown in equations 57-60 gives

$$P_{0A} = -2\lambda M_1 [E_I (1 - A_{\lambda}) + E_{II} (1 + A_{\lambda})] \quad (97)$$

$$P_{0B} = -2\lambda M_1 [E_I (1 - A_{\lambda}) - E_{II} (1 + A_{\lambda})] \quad (98)$$

$$M_{0A} = 2M_1 [E_I (1 - D_{\lambda}) + E_{II} (1 + D_{\lambda})] \quad (99)$$

$$M_{0B} = 2M_1 [E_I (1 - D_{\lambda}) - E_{II} (1 + D_{\lambda})]. \quad (100)$$

Substituting into the deflection and moment formulas for a single concentrated point force, equations 40 and 42, and a single concentrated moment, equations 45 and 47, found earlier, the deflections for the end-conditioning forces are shown to be

$$y(P_{0A}) = -\frac{M_1 \lambda^2}{k} [E_I (1 - A_{\lambda}) + E_{II} (1 + A_{\lambda})] A_{\lambda x} \quad (101)$$

$$y(P_{0B}) = -\frac{M_1 \lambda^2}{k} [E_I (1 - A_{\lambda}) - E_{II} (1 + A_{\lambda})] A_{\lambda x} \quad (102)$$



$$y(M_{0A}) = \frac{2M_1\lambda^2}{k} [E_I(1 - D_{\lambda}) + E_{II}(1 + D_{\lambda})] B_{\lambda x} \quad (103)$$

$$y(M_{0B}) = \frac{2M_1\lambda^2}{k} [E_I(1 - D_{\lambda}) - E_{II}(1 + D_{\lambda})] B_{\lambda x} \quad (104)$$

Adding the deflections in equations 101-104 together gives the deflection formula for a finite beam on an elastic foundation with free ends, loaded with a moment load on one end as

$$y = \frac{2M_1\lambda^2}{k} [2E_I(1 - D_{\lambda})B_{\lambda x} - E_I(1 - A_{\lambda})A_{\lambda x}] \quad (105)$$

where  $M_1$  is the applied moment load

The moments for the end-conditioning forces are found to be

$$M(P_{0A}) = -\frac{M_1}{2} [E_I(1 - A_{\lambda}) + E_{II}(1 + A_{\lambda})] C_{\lambda x} \quad (106)$$

$$M(P_{0B}) = -\frac{M_1}{2} [E_I(1 - A_{\lambda}) - E_{II}(1 + A_{\lambda})] C_{\lambda x} \quad (107)$$

$$M(M_{0A}) = M_1 [E_I(1 - D_{\lambda}) + E_{II}(1 + D_{\lambda})] D_{\lambda x} \quad (108)$$

$$M(M_{0B}) = M_1 [E_I (1 - D_{\lambda}) - E_{II} (1 + D_{\lambda})] D_{\lambda x} \quad (109)$$

Adding equations 106-109 together, the moment formula is

$$M = 2M_1 E_I [(1 - D_{\lambda}) D_{\lambda x} - (1 - A_{\lambda}) C_{\lambda x}]. \quad (110)$$

The use of trigonometric functions allows equations 83, 88, 105 and 110 to be presented in another form. The notation for the applied loads will be changed from  $P_1$  and  $M_1$  to  $P$  and  $M_0$ . In the case of a shear loading on the end of the cylinder, shown in Figure 3 as applied to a beam on an elastic foundation, the deflection,  $y$ , and moment,  $M$ , respectively are [7]

$$y = \frac{2P\lambda \sinh \lambda l \cos \lambda x \cosh \lambda x' - \sin \lambda l \cosh \lambda x \cos \lambda x'}{k (\sinh^2 \lambda l - \sin^2 \lambda l)} \quad (111)$$

$$M = \frac{-P \sinh \lambda l \sin \lambda x \sinh \lambda x' - \sin \lambda l \sinh \lambda x \sin \lambda x'}{\lambda (\sinh^2 \lambda l - \sin^2 \lambda l)} \quad (112)$$

where  $P$  is the applied shear load

In the case of a moment loading on the end of the cylinder, shown in Figure 4 as applied to a beam on an elastic foundation, the deflection,  $y$ , and moment,  $M$ , respectively are [7]

$$y = \frac{2M_0\lambda^2}{k} \frac{1}{\sinh^2 \lambda l - \sin^2 \lambda l} \left[ \frac{\sinh \lambda l (\cosh \lambda x' \sin \lambda x - \sinh \lambda x' \cos \lambda x)}{\sinh \lambda l (\sinh \lambda x \cos \lambda x' - \cosh \lambda x \sin \lambda x')} \right] \quad (113)$$

$$M = M_0 \frac{1}{\sinh^2 \lambda l - \sin^2 \lambda l} \left[ \frac{\sinh \lambda l (\sinh \lambda x' \cos \lambda x + \cosh \lambda x' \sin \lambda x)}{-\sin \lambda x (\sinh \lambda x \cos \lambda x' + \cosh \lambda x \sin \lambda x')} \right] \quad (114)$$

where  $M_0$  is the applied moment.

For cylindrical shell applications [5], a longitudinal element of the cylinder is removed and treated as a beam on an elastic foundation. In this type of application

$$k = \frac{Et}{R_m^2} \quad (115)$$

is the beam modulus  $k$ , where  $E$  is the modulus of elasticity,  $t$  is the shell thickness and  $R_m$  is the mean radius. The characteristic,  $\lambda$ , for the cylindrical body is

$$\lambda = \sqrt[4]{\frac{k}{4EI}} \quad (116)$$

where the moment of inertia,  $I$ , is

$$I = \frac{t^3}{12(1-\mu^2)} \quad (117)$$

The mean radius  $R_m$  is found by the equation

$$R_m = \frac{R_I + R_O}{2} \quad (118)$$

The conventional thin shell longitudinal [8] and circumferential [5] stresses,  $\sigma_L$  and  $\sigma_C$ , respectively, are calculated using the formulas

$$\sigma_L = \frac{6M}{t^2} \quad (119)$$

$$\sigma_C = -\frac{Ey}{R_m} \pm \sigma_L \mu \quad (120)$$

The plus and minus signs in the formula for  $\sigma_C$  give the fiber stresses at the inside and at the outside surface of the cylinder respectively. Tensile stress is always regarded as positive.

### **Solutions using thick cylinder corrections.**

Equations 117 and 118 for the moment of inertia,  $I$ , and the mean radius,  $R_m$ , are intended for use with thin cylinders. As shown in Figure 10, for thick

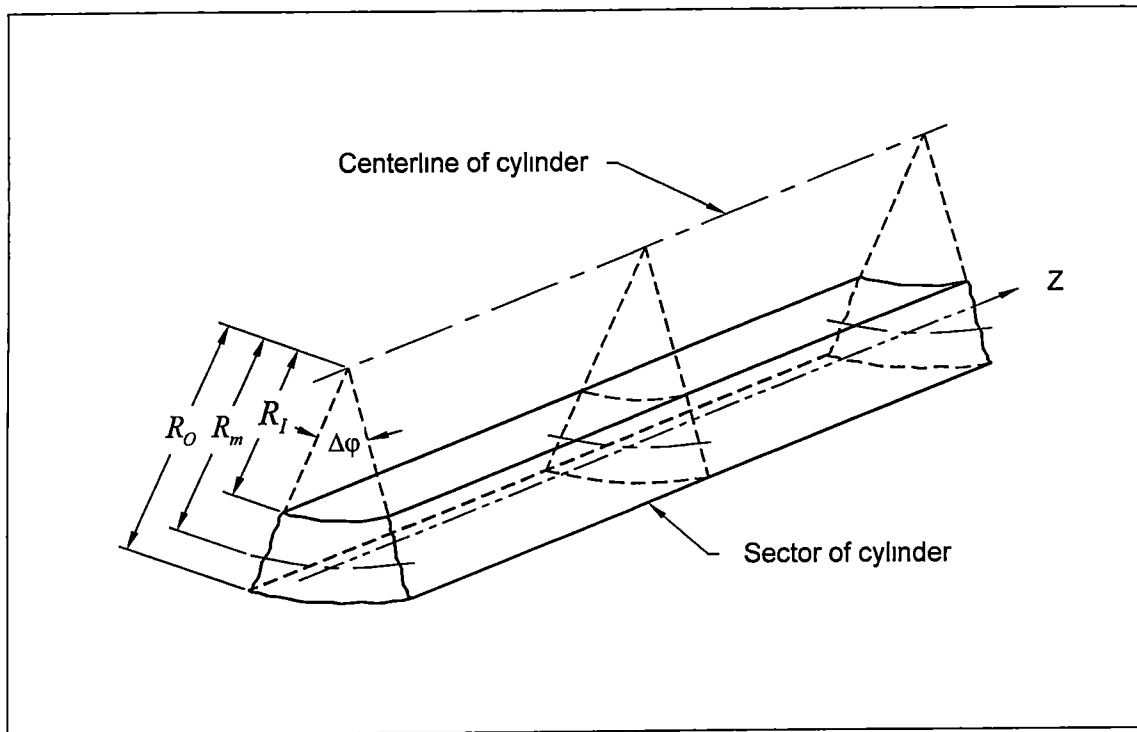


**Figure 10.** A sector removed from a cylinder that is to be analyzed using beam on elastic foundation [6]

cylinders, a sector is removed and analyzed as a beam on an elastic foundation. The neutral axis location is shifted farther away from the thin cylinder mean radius and closer to the outside radius of the cylinder. A more accurate solution may be obtained for thicker cylinders if the moment of inertia and mean radius are corrected to account for this shift. The thick cylinder formula for the area moment of inertia for the sector about the neutral axis,  $I$ , is

$$I = \left\{ \frac{3 \left[ \left( \frac{R_O}{R_I} \right)^4 - 1 \right] \left[ \left( \frac{R_O}{R_I} \right)^2 - 1 \right]}{8 \left[ \left( \frac{R_O}{R_I} \right)^3 - 1 \right]} - \frac{1}{3} \left[ \left( \frac{R_O}{R_I} \right)^3 - 1 \right] \right\} R_I^3 \quad [6] \quad (121)$$

where  $R_o$  and  $R_i$  are the outside and inside radii respectively. The radius at which the neutral axis is located on the sector is

$$R_m = \frac{2 \left( \frac{R_o}{R_i} \right)^3 - 1}{3 \left( \frac{R_o}{R_i} \right)^2 - 1} R_i \quad [6] \quad (122)$$

The characteristic  $\lambda$  must be corrected for the stiffening effect due to the axial symmetry of the cylindrical shell by increasing the moment of inertia by a factor of  $\frac{1}{1-\mu^2}$ , or

$$\lambda = \sqrt[4]{\frac{k(1-\mu^2)}{4EI}}. \quad (123)$$

The longitudinal stress is found by using the preceding thick shell modifications for the moment of inertia and the mean radius and is given by the formula

$$\sigma_L = \frac{Mc}{I} = \frac{M(R-R_m)}{I} \quad [6] \quad (124)$$

where  $R$  is the radius at the point of interest, which in this case is either the inner

or outer radius. This value is limited to the range of  $R_I$  to  $R_O$ . The bending moment  $M$  in equation 124 is applied about the neutral axis of the sector.

### Classification of beams.

It is important to note that beams, based on their length and their  $\lambda$ , may be classified into three categories [9] as follows.

- I. Short beams:  $\lambda < \frac{\pi}{4}$ ;
- II. Beams of medium length:  $\frac{\pi}{4} < \lambda < \pi$ ;
- III. Long beams:  $\lambda > \pi$

These classifications are based on stiffness and allow approximations to be made and certain terms may be neglected in the beam on an elastic foundation equations. Beams in Category I can be assumed to be absolutely rigid so that the bending in the beam may be neglected, only rotation needs to be considered and simple statics will give a satisfactory solution. Category II requires an accurate use of the beam on an elastic foundation equations 111-114 since the assumption is that a force acting on one end of the beam has an effect at the other end of the beam. Beams belonging to Category III are assumed to be long, therefore, a force at one end of the beam is assumed to have a negligible effect on the other end of the beam. Because of this assumption, certain terms in the equations may be taken as zero. These assumptions can greatly simplify the calculations. For a long beam in Category III,  $A_\lambda$ ,  $B_\lambda$ ,  $C_\lambda$ , and  $D_\lambda$  may be

taken as zero in the beam on elastic foundation equations 83, 88, 105, and 110  
 The simplified form of the equations for deflection and moment for long beams in  
 Category III for an end shear load as shown in Figure 3 in this chapter are

$$y = \frac{2P_1\lambda}{k} \cos \lambda x (\cosh \lambda x - \sinh \lambda x) \quad (125)$$

$$M = -\frac{P_1}{\lambda} \sin \lambda x (\cosh \lambda x - \sinh \lambda x) \quad (126)$$

where  $P_1$  is the applied shear load. Equations for the deflection and moment for  
 a moment load applied to the end of a beam as shown in Figure 4 in this chapter  
 are

$$y = \frac{2M_1\lambda^2}{k} (\cosh \lambda x - \sinh \lambda x) (\sin \lambda x - \cos \lambda x) \quad (127)$$

$$M = M_1 (\cosh \lambda x - \sinh \lambda x) (\cos \lambda x + \sin \lambda x) \quad (128)$$

where  $M_1$  is the applied moment load.

For this study, the finite length equations 111-114 (formulas for medium  
 length beams of Category II) are used for all calculations. The deflections and  
 moments are calculated for the inner and outer radii of the cylinder down the  
 entire length. These values are then used to find the longitudinal and



circumferential stresses These stresses are then compared to the finite element solution

## CHAPTER 3

### FINITE ELEMENT ANALYSIS

#### **Description of method.**

Next, the cylinder geometries are analyzed using the finite element method. The program used is Algor®. The edge loads were applied in several different ways and the results were used to determine a Saint-Venant's length, as defined on page 3, for each cylinder. Details of how this length was determined are presented at the end of this chapter. Taking this Saint-Venant's length into account, the results are compared to the results obtained from the beam on an elastic foundation analysis for the circumferential and longitudinal stresses.

#### **Element type and mesh density.**

Since the geometry of a cylinder is symmetrical and the loading situations are symmetrical around the top surfaces of the cylinders, axisymmetric elements were used. The orientation of these elements is shown in Figure 11. Within Algor®, axisymmetric elements are classed as 2-dimensional solid elements. Brick elements could also have been used, however, for the same mesh density, there are many fewer axisymmetric elements. This element also has fewer degrees of freedom and a simpler formulation than the brick element. All of this serves to drastically reduce the problem size. "A reduction of two orders of magnitude in the problem run time with no reduction in accuracy of the result is typical." [10]

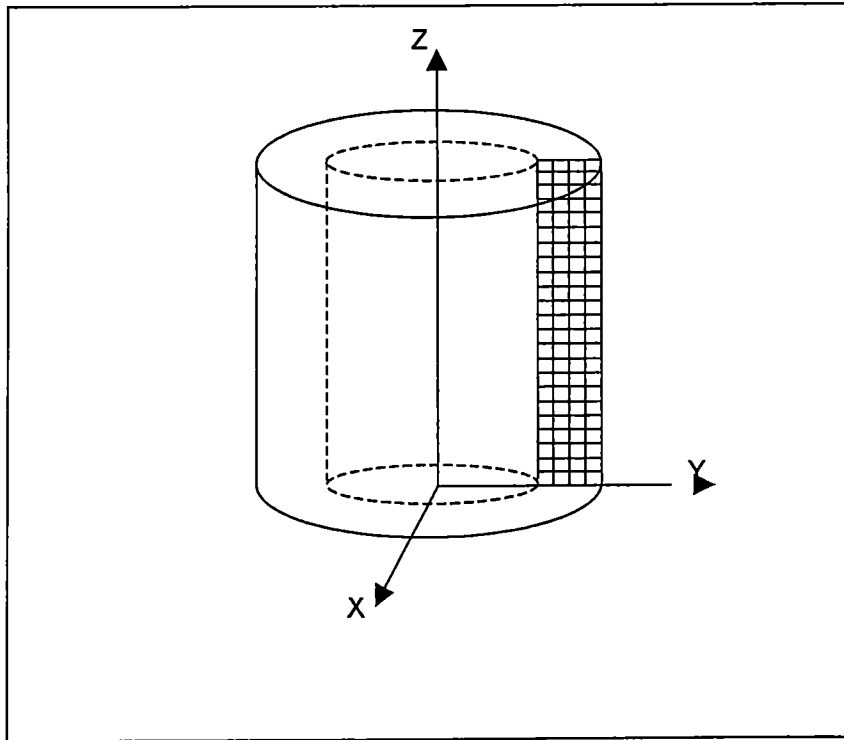


**Figure 11.** Axisymmetric elements and coordinate system

Mesh density for each cylinder geometry analyzed is shown in Table 1. A measure within Algor® called Precision [18] was used to verify the accuracy of the mesh density. The Precision value is defined as

$$\frac{0.5(\text{MaxvonMises} - \text{MinvonMises})}{\text{GlobalvonMisesMaximum}} \quad (129)$$

The Max von Mises and Min von Mises stresses are the highest and lowest stress values computed by any element at a given node. This quantity is computed at each node and may range from 0 to 0.5 with 0 indicating perfect agreement of the stress values and 0.5 indicating no agreement. If the Precision

**Table 1** Cylinder geometries and mesh densities Each cylinder was analyzed for two lengths, 15.0" and 7.5"

OD	ID	WALL THICKNESS	R/t	ELEMENT SIZE	MESH DENSITY HORIZONTAL	MESH DENSITY VERTICAL	
						15.0" Long	7.5" Long
15.0"	5.0"	5.0"	1.0	0.125"	40	120	60
15.0"	8.75"	3.125"	1.9	0.125"	25	120	60
15.0"	10.0"	2.5	2.5	0.0625"	40	240	120
15.0"	11.0"	2.0"	3.25	0.0625"	32	240	120
15.0"	12.5"	1.25	5.5	0.03125"	40	480	240
15.0"	13.5"	0.75"	9.5	0.025"	30	600	300
15.0"	14.0"	0.5"	14.5	0.0125"	40	1200	600
15.0"	14.25"	0.375"	19.5	0.0125"	30	1200	600
15.0"	14.625"	0.1875"	39.5	0.00625"	30	2400	1200
15.0"	14.75"	0.125"	59.5	0.00625"	20	2400	1200

value is less than 0.05, it is unlikely that refining the mesh density will significantly effect the stress values [18] The mesh densities used for this study were well within this range

**Loading and boundary conditions.**

Both the shear and moment loads were applied using point forces. The forces were applied to the nodes on the top surfaces of the cylinders in several different ways to provide a wide range of loading situations, as shown in Figure 12 for shear and Figure 13 for moment

The boundary condition applied to the model is a restriction from movement in the vertical direction The condition is applied near the neutral axis on the bottom surface of the cylinder model to minimize any constraint influence

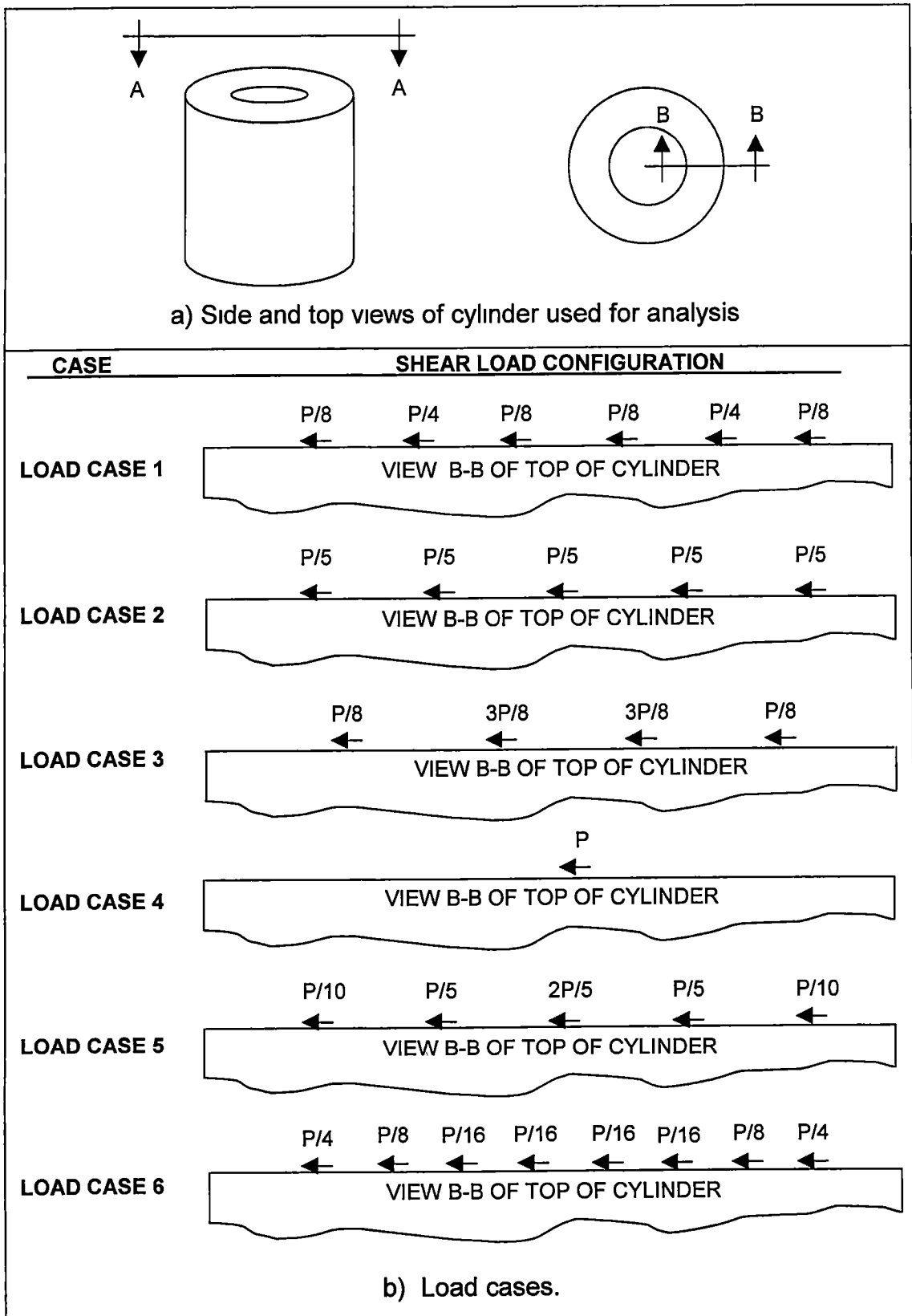


Figure 12. Load cases for shear loading, P, for 15 0" and 7 5" cylinders

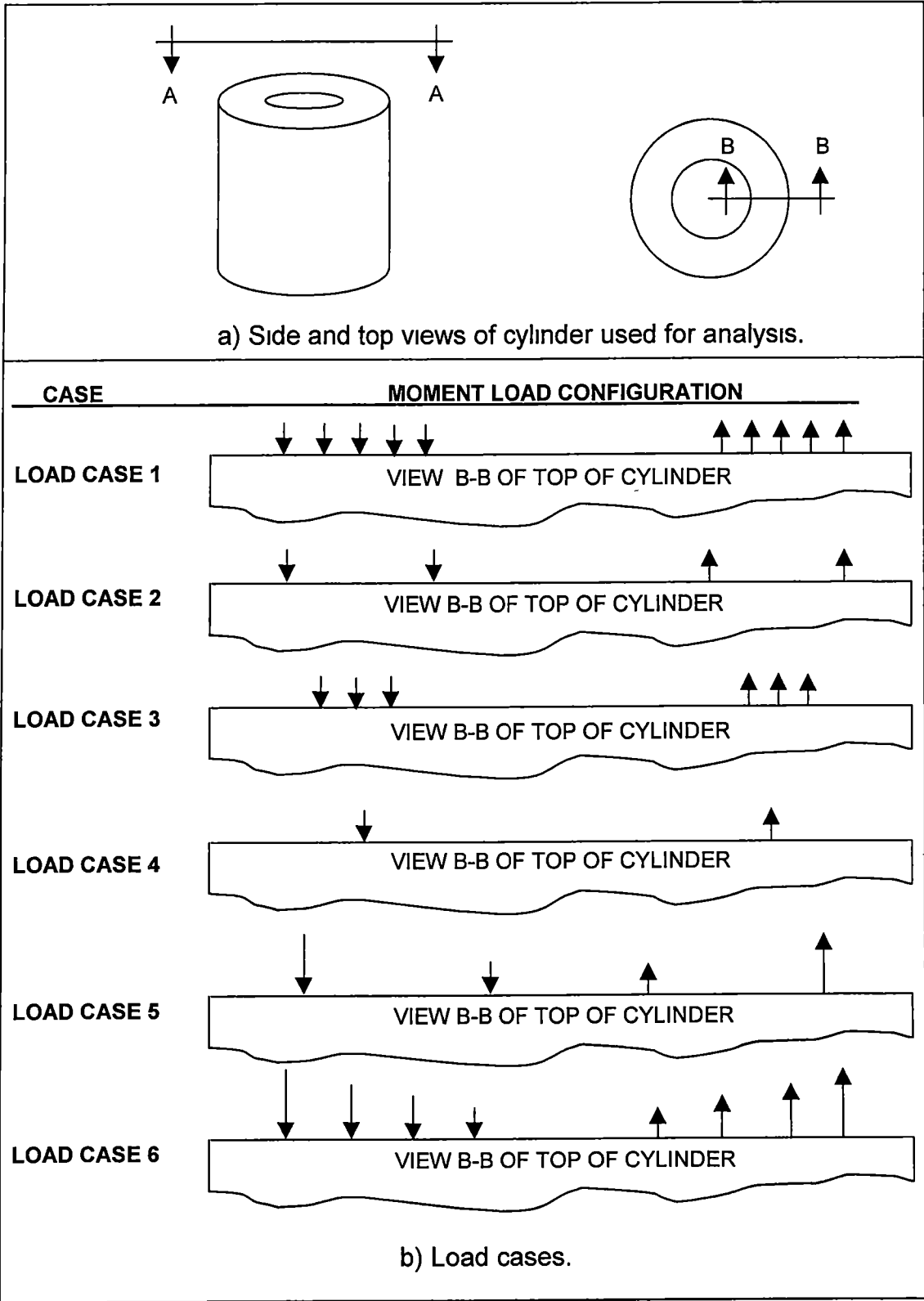


Figure 13. Load cases for moment loading, M, for 15 0" and 7 5" cylinders

### **Other specifics used in the analysis.**

The vector stresses in the vertical (Z) and cylindrical (X) directions are computed and output to a file, representing the longitudinal and the circumferential stresses respectively. These stresses are taken on the inner and outer radii starting at the load and continuing down the length of the cylinder. The orientation of the coordinate system is shown in Figure 11. The stress values represent the average of the values computed by each element at each node and the cylinder material is assumed to be epoxy-plastic with a Modulus of Elasticity ( $E$ ) of 500,000 psi and a Poisson's Ratio ( $\mu$ ) of 0.375.

### **Saint-Venant's length.**

The Saint-Venant's length was found for each cylinder geometry by taking the six different load cases for the shear and six moment load configurations applied to the cylinder and comparing them to see when the stresses converge to within a standard deviation of 0.005 or less. An example of the converging stresses is given in Figure 14 for an end moment load on a 15.0" OD, 11.0" ID, 15.0" long cylinder. The stress divided by the load is plotted versus the distance from the load for the entire length of the cylinder. It is plainly seen that the method of loading has an effect on the stresses at a distance close to where the load is applied.

The formula for standard deviation [11]

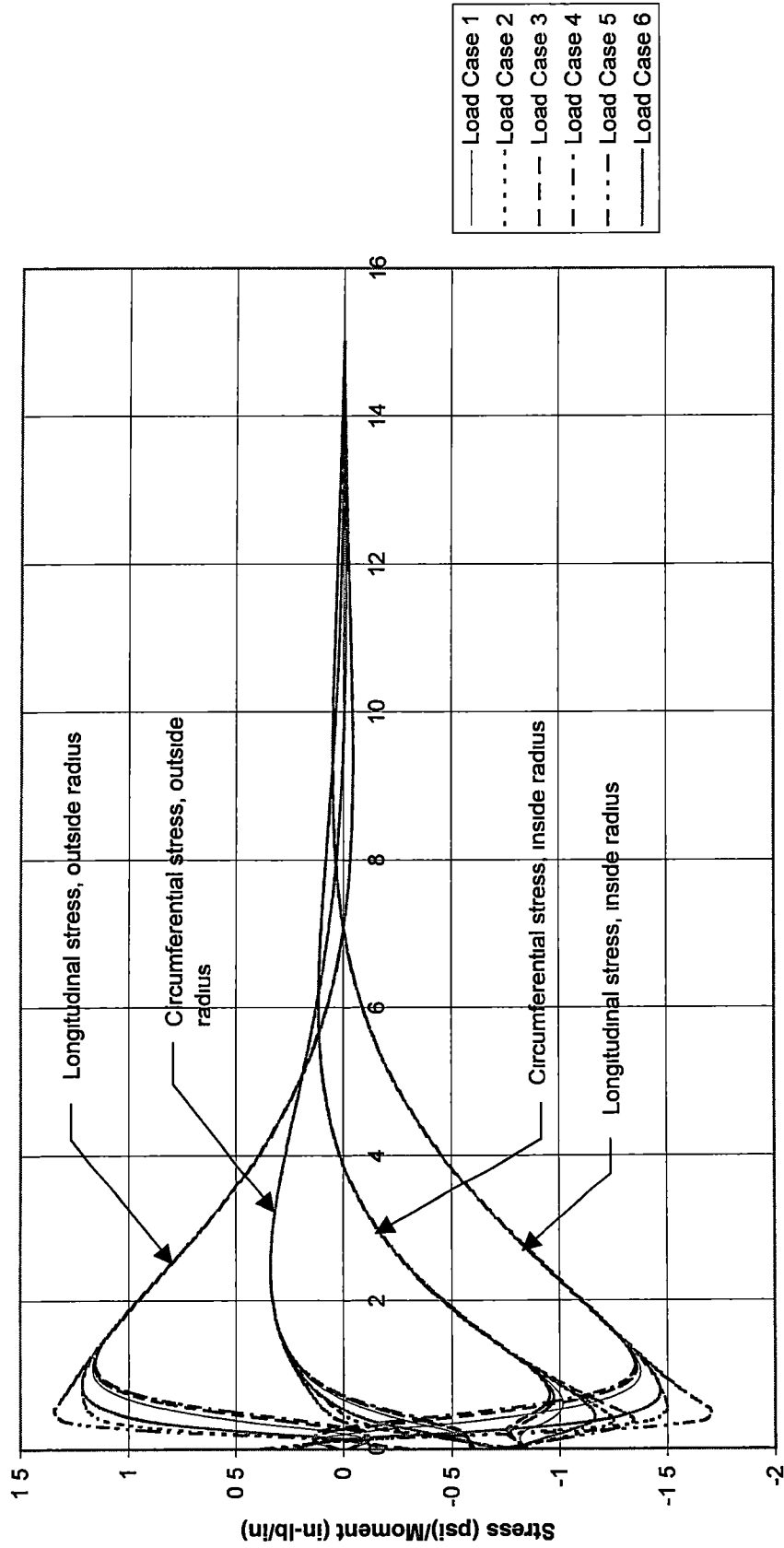


Figure 14. Stress divided by load vs. distance from load for moment load on 15.0" OD, 11.0" ID, 15.0" long cylinder. Stresses are taken from finite element solution to determine the Saint-Venant's length. Reference Figure 13, p. 42 for load cases.



$$S.D. = \sqrt{\frac{\sum x_i^2 - n(\bar{x})^2}{n-1}} \quad (130)$$

is used to provide an estimate of the range of stress values at a single point on the surface of the cylinder given by the six cases. In this formula  $x_i$  represents the stress values,  $n$  is the number of data points, and  $\bar{x}$  is the arithmetic mean as follows

$$\bar{x} = \frac{x_1 + x_2 + \dots + x_n}{n} = \frac{\sum x_i}{n} \quad (131)$$

A Saint-Venant's length was found for the shear and for the moment load cases and then the two lengths were combined into one Saint-Venant's length by taking the more conservative of the two. The length was taken at a standard deviation of 0.005 or less. This was done for each cylinder geometry.

## CHAPTER 4

### COMPARISON OF DATA

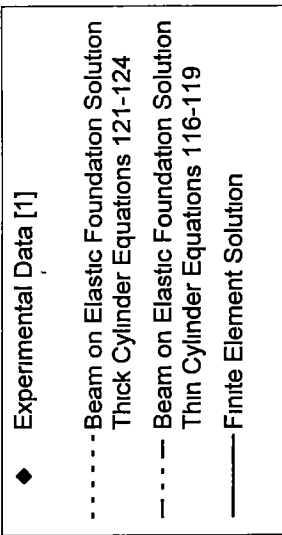
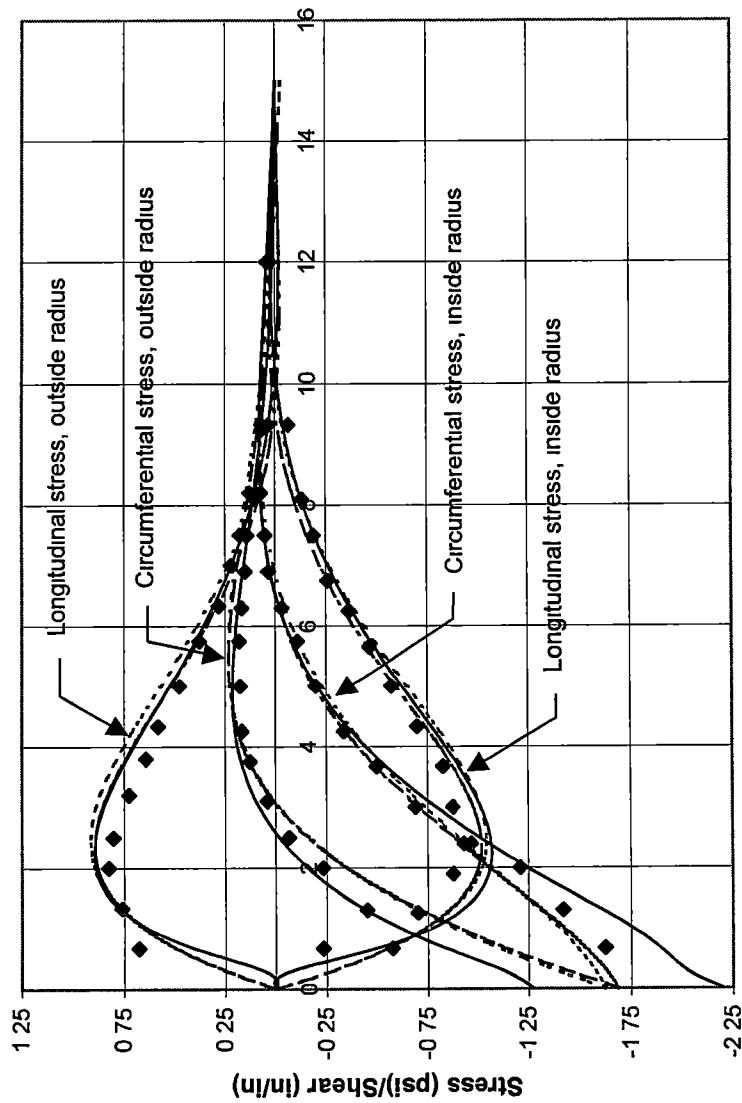
#### **Comparison of results with experimental data.**

Figures 15-18 compare the beam on elastic foundation and finite element results with the experimental data obtained by Dohrmann and Ives' [1]. The cylinder geometry is 15.0" OD and 10.0" ID. Both shear and moment load cases are shown for the 15.0" and 7.5" long cylinders. The material is epoxy-plastic with a moment of inertia  $I$  of 500,000 psi and a Poisson's Ratio  $\mu$  of 0.375. Stress divided by the load vs. distance from the load for both longitudinal and circumferential stresses are compared.

#### **Comparison of analysis techniques for 15.0" and 7.5" cylinders.**

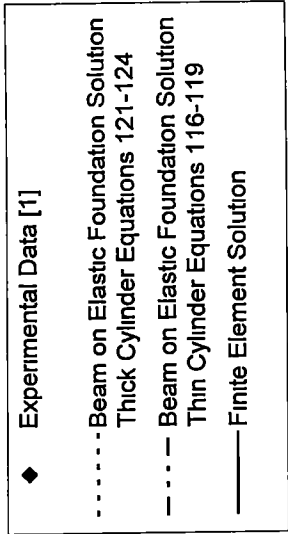
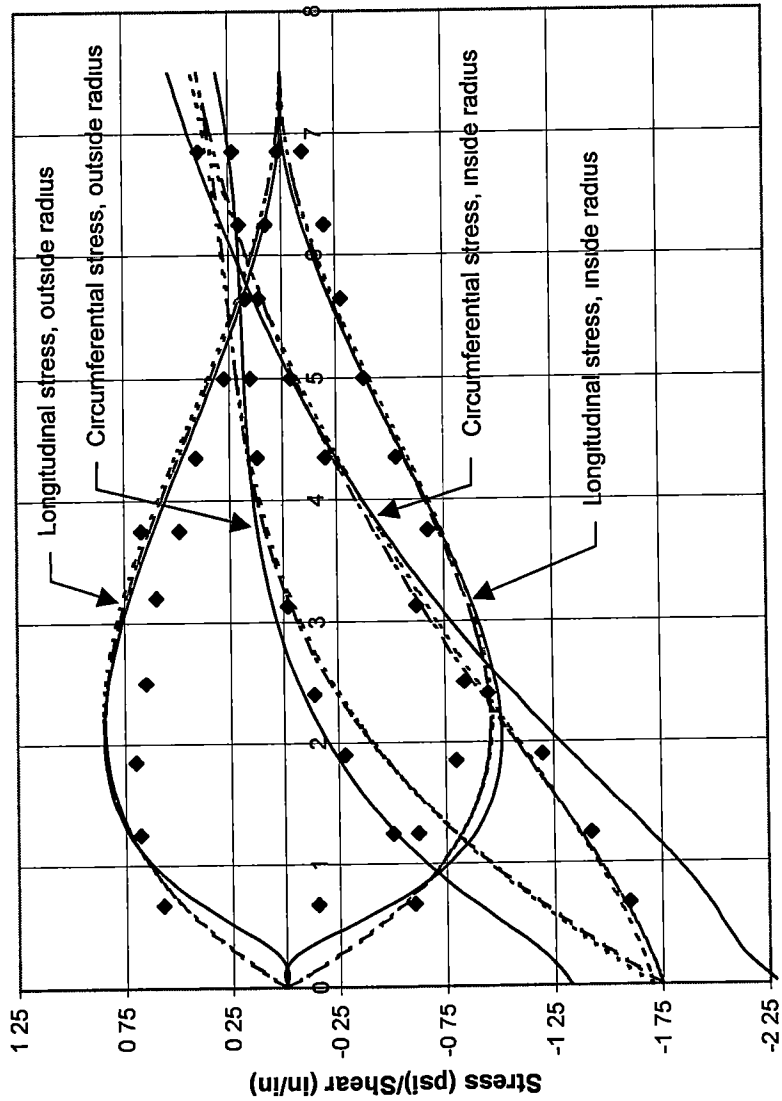
This chapter also provides a comparison of a beam on an elastic foundation analysis and a finite element analysis shown in the form of percent error vs.  $R/t$ . The analyses provided values of the longitudinal and circumferential stresses on the surfaces of each cylinder. Also, the influence of the Saint-Venant's length as it relates to the  $R/t$  ratio is shown.

In order to find the percent error between the two analysis methods, the finite element method was assumed to be the correct solution. The error between the finite element solution and the beam on an elastic foundation solution is



Distance From Load (in)

Figure 15. Stress divided by load vs. distance from load for shear load on 15.0" OD, 10.0" ID, 15.0" long cylinder.



Distance From Load (in)

Figure 16. Stress divided by load vs. distance from load for shear load on 15.0" OD, 10.0" ID, 7.5" long cylinder.

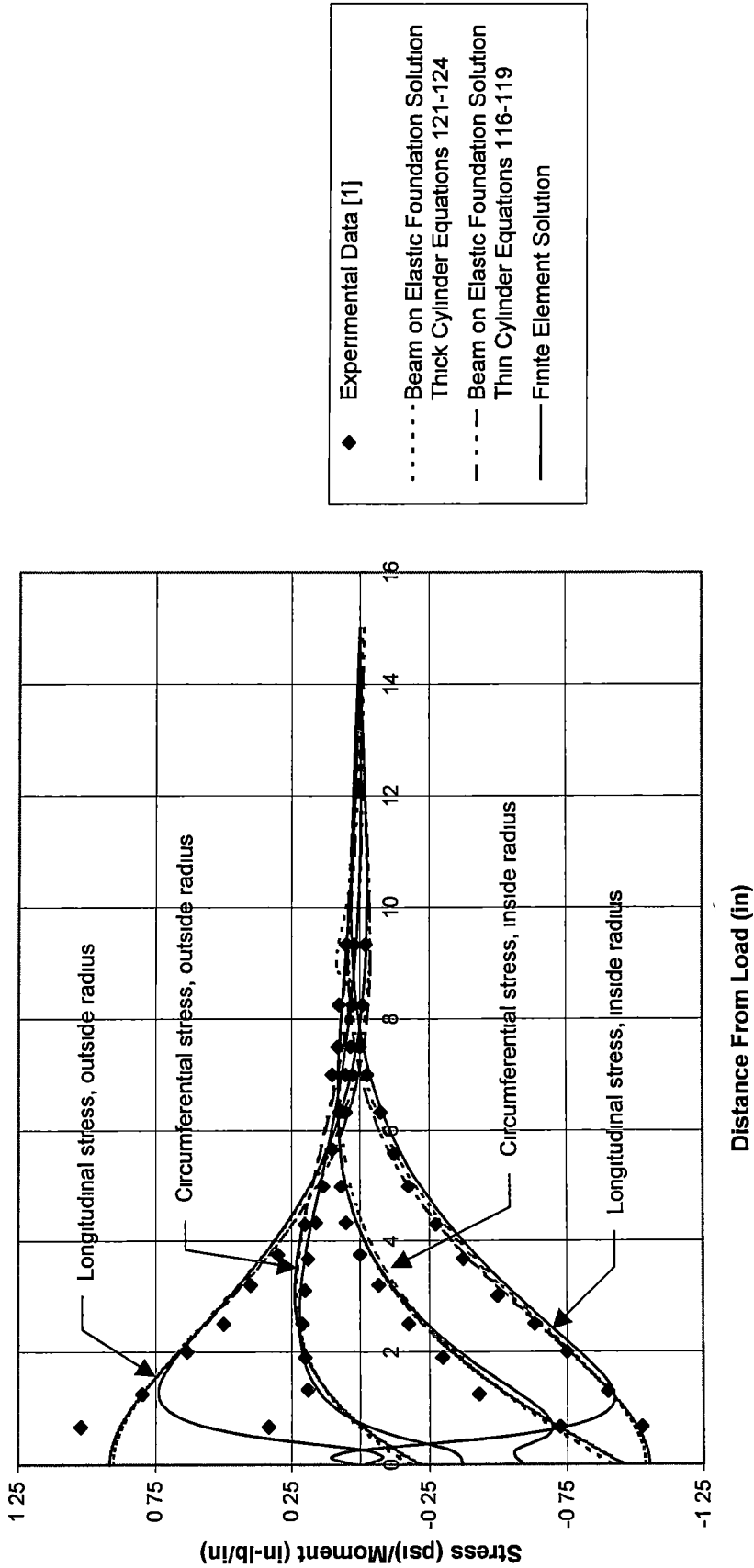
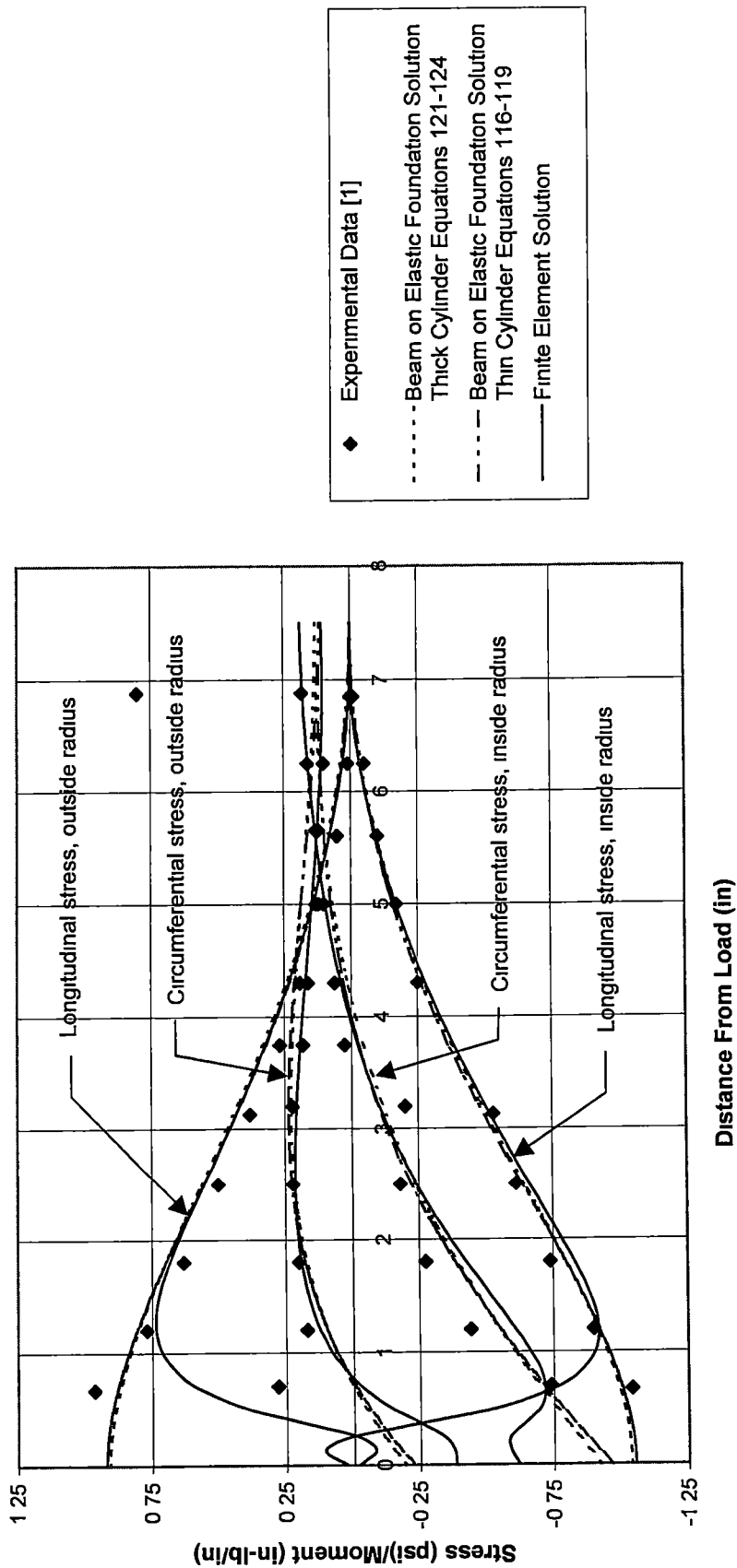


Figure 17. Stress divided by load vs. distance from load for moment load on 15.0" OD, 10.0" ID, 15.0" long cylinder.



Distance From Load (in)

Figure 18. Stress divided by load vs. distance from load for moment load on 15.0" OD, 10.0" ID, 7.5" long cylinder.

$$\%error = \frac{FiniteElementSolution - BeamOnAnElasticFoundationSolution}{FiniteElementSolution} \times 100 \quad (132)$$

The maximum stress was found using the finite element solution at a distance from the load greater than the Saint-Venant's length for each cylinder geometry. The percent error between the two solutions was then found at that point. The percent errors were then averaged for the six different loading cases for moment and shear.

Refer to Table 1 in Chapter 3 for the cylinder geometries which have been analyzed along with their  $R/t$  ratios. For each geometry, two lengths were analyzed, 7.5" and 15.0". Figures 12 and 13 in Chapter 3 show the shear and moment load configurations used for each cylinder geometry. Figures 19 and 20 show the influence of the Saint-Venant's length and Figures 21 through 24 show the behavior of the percent error between the finite element solution and the beam on elastic foundation solution using both thin shell formulas and thick shell corrections.

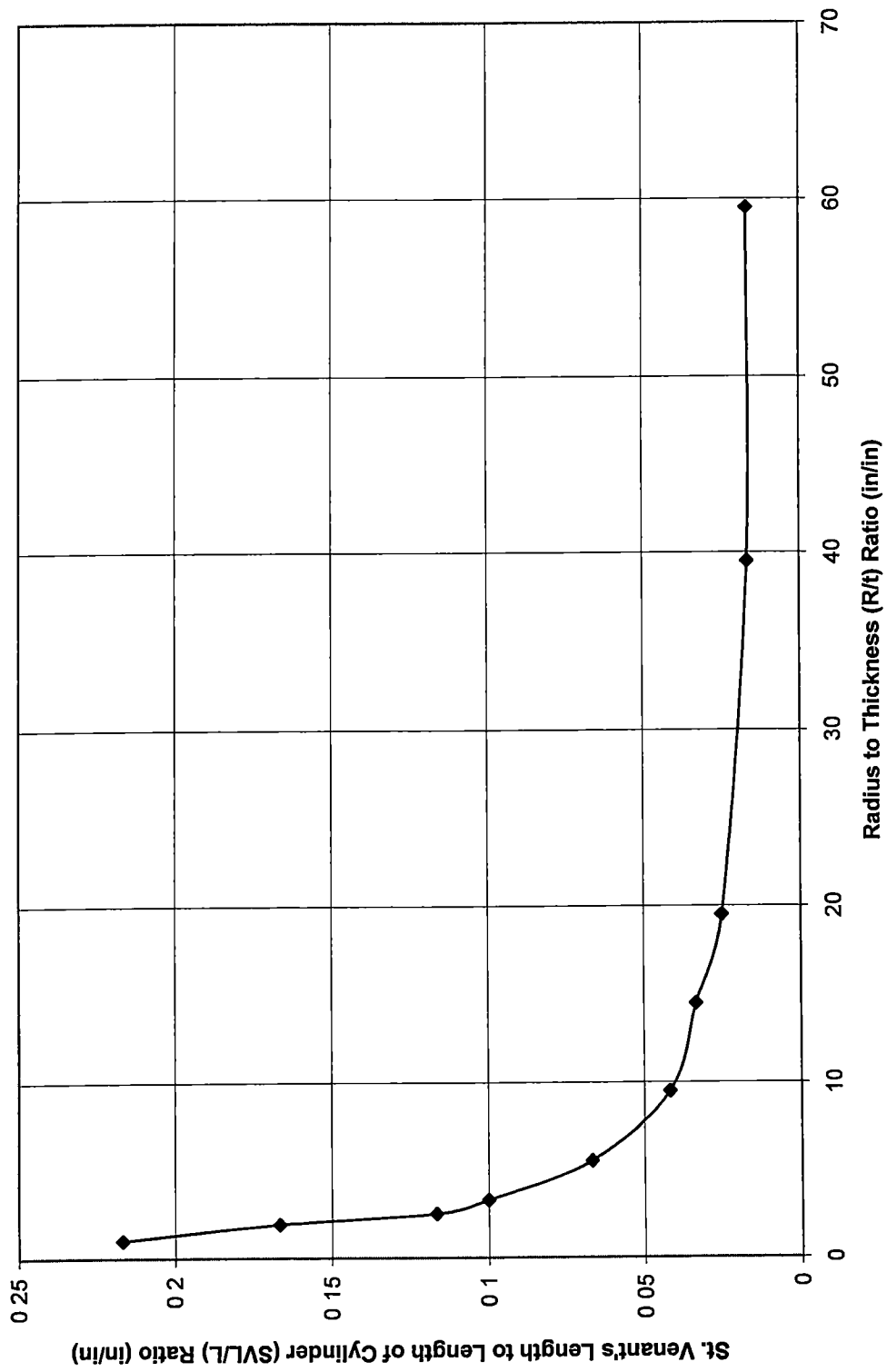


Figure 19. St. Venant's length divided by length of cylinder vs. radius to thickness (R/t) ratio for 15.0" cylinders.



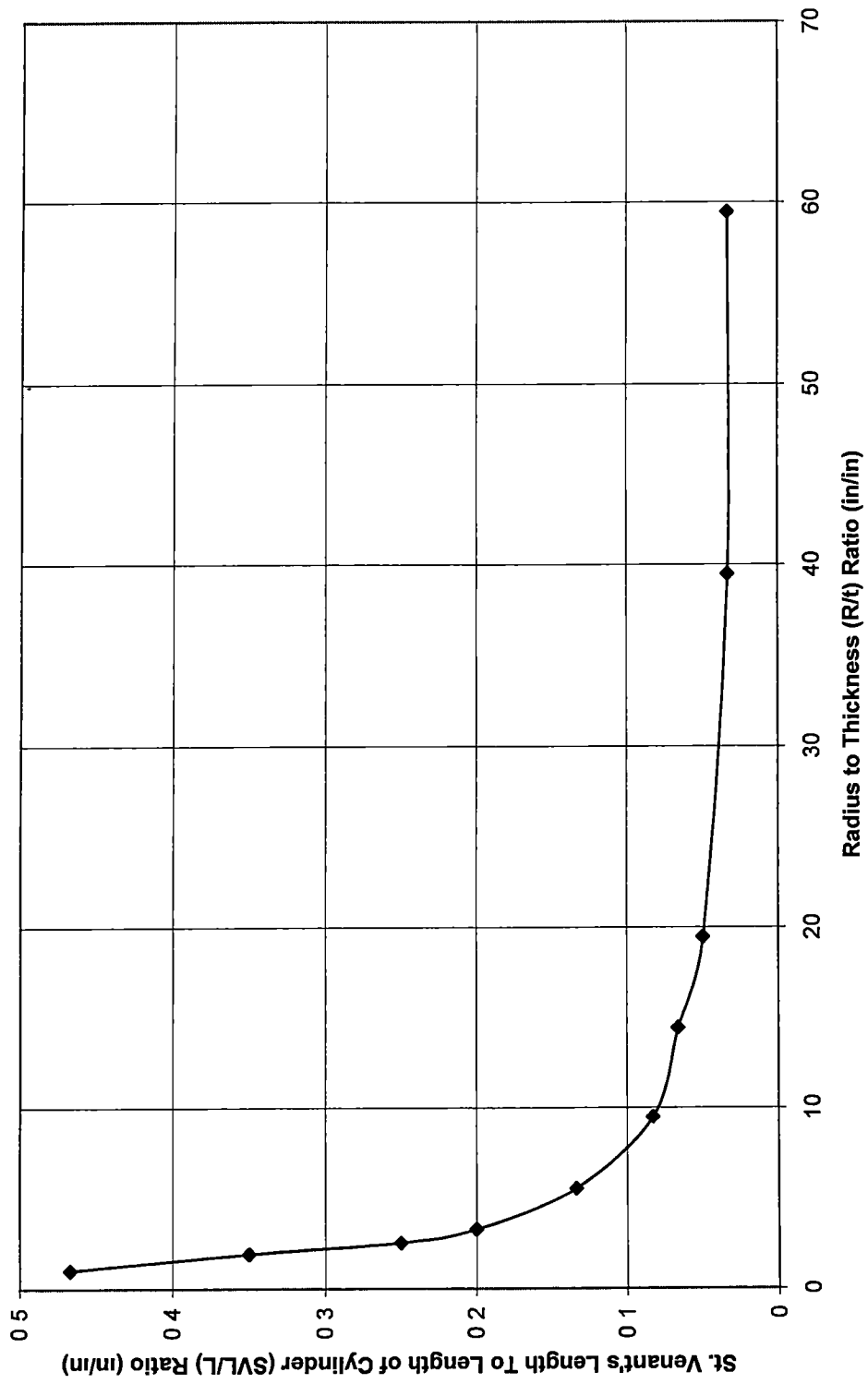
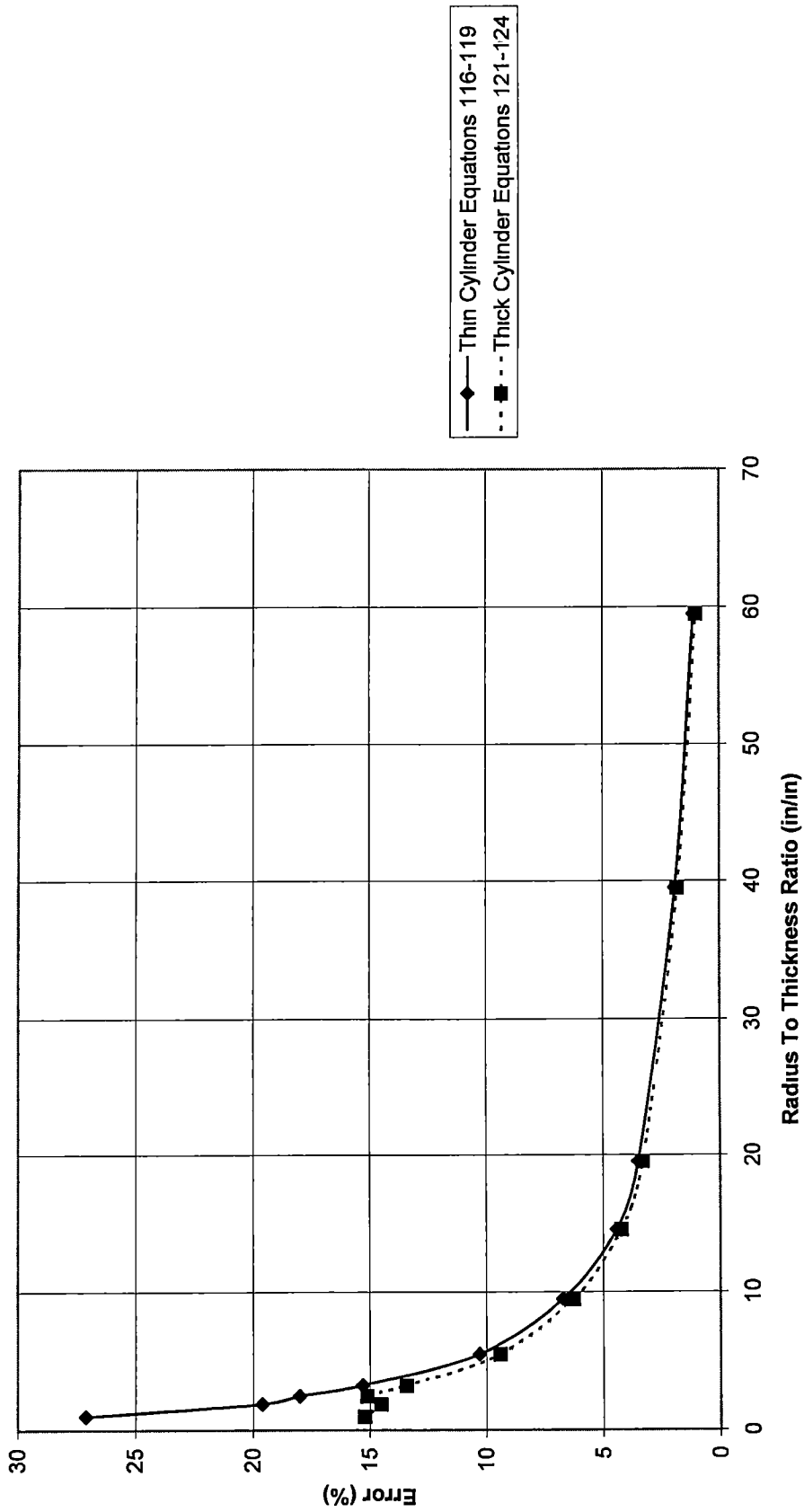
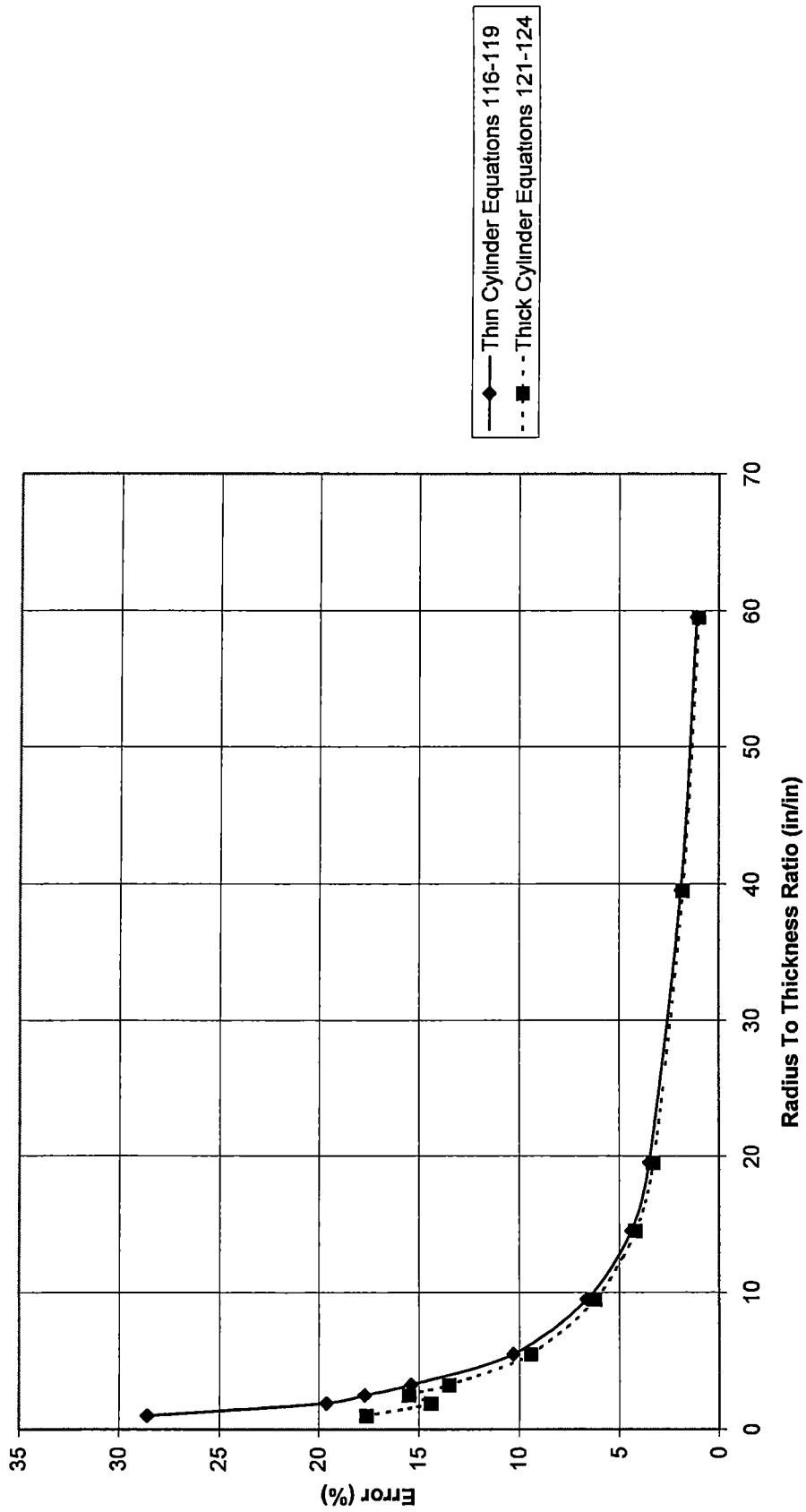


Figure 20. St. Venant's length divided by length of cylinder vs. radius to thickness (R/t) ratio for 7.5" cylinders.



**Figure 21. Percent error vs. radius to thickness ratio between finite element results and beam on elastic foundation results for shear load on 15.0" cylinders.**



**Figure 22. Percent error vs. radius to thickness ratio between finite element results and beam on elastic foundation results for shear load on 7.5" cylinders.**

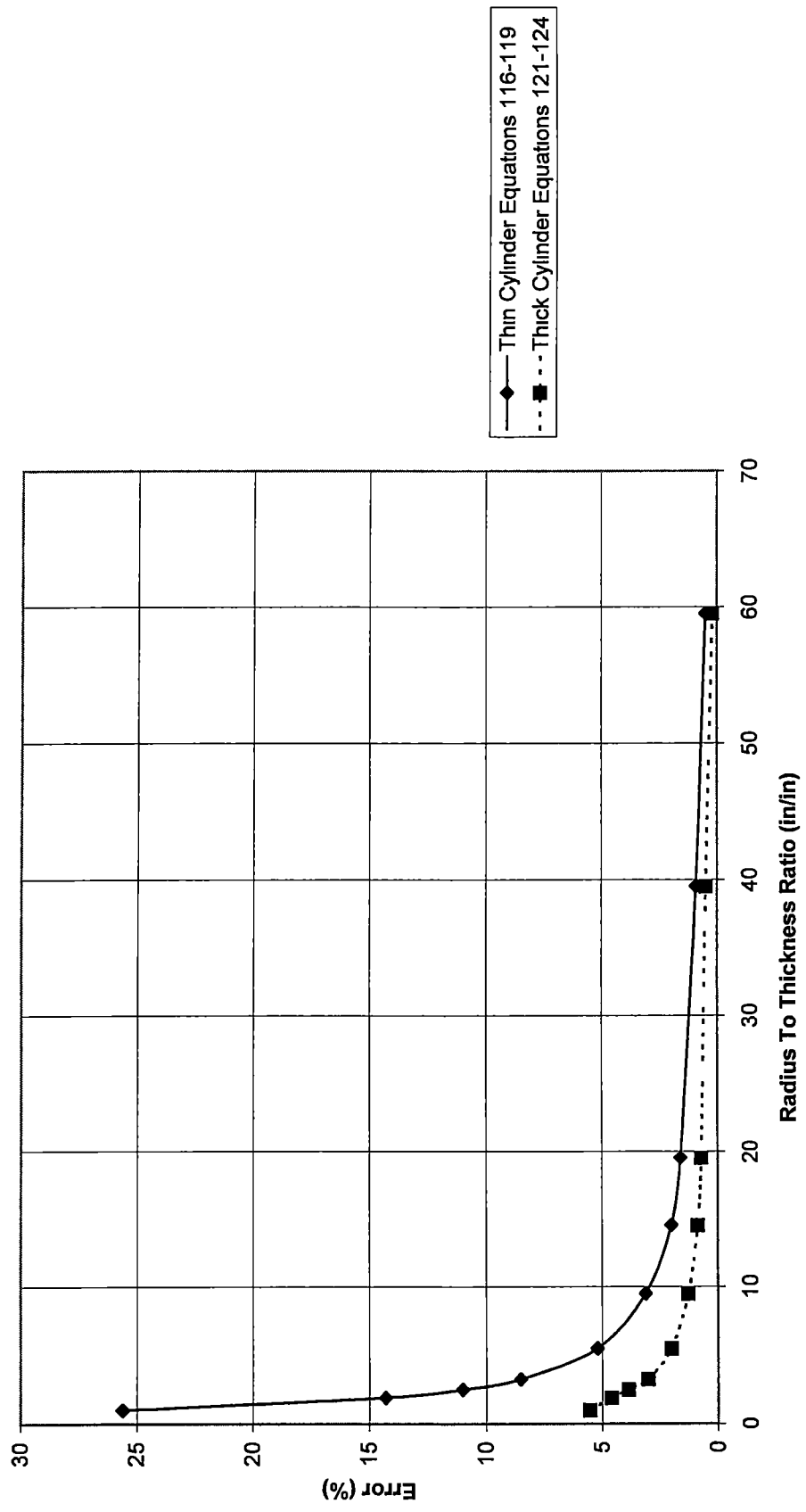


Figure 23. Percent error vs. radius to thickness ratio between finite element results and beam on elastic foundation results for moment load on 15.0" cylinders.

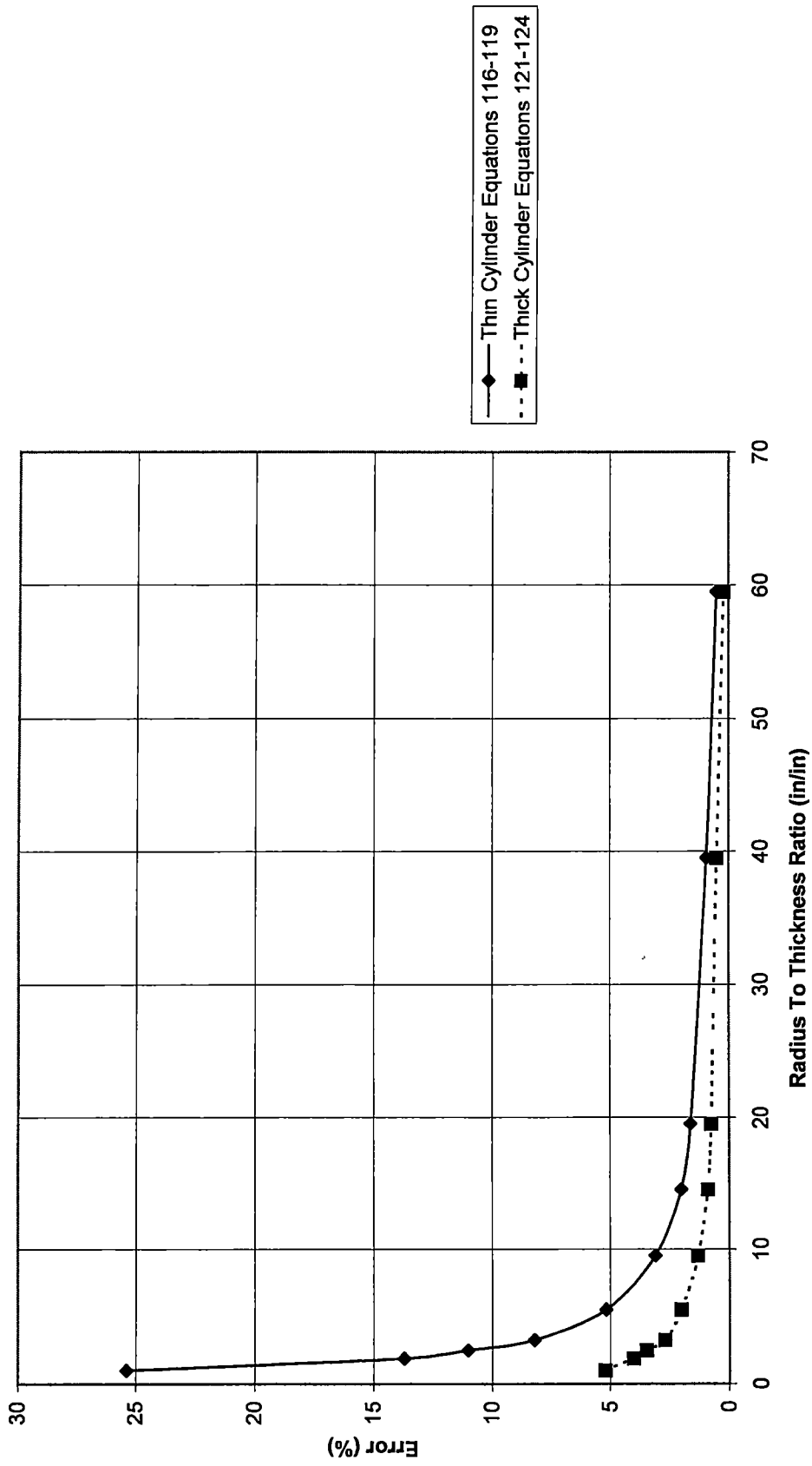


Figure 24. Percent error vs. radius to thickness ratio between finite element results and beam on elastic foundation results for moment load on 7.5" cylinders.

## CHAPTER 5

### CONCLUSIONS

#### **Experimental data.**

The stress divided by the load versus the distance from the load is shown in Figures 15-18 in Chapter 4 for Dohrmann's and Ives' experimental data [1], the finite element solution, and the beam on an elastic foundation solution for the 15.0" OD, 10.0" ID cylinder geometry used in the experiment. Both shear and moment loadings are represented for both 15.0" and 7.5" long cylinders.

Figures 15 and 16 show the comparisons for the shear loading. Both the 15.0" and 7.5" long cylinders tend to show the same trend. The experimental longitudinal stresses were slightly less than those predicted by the beam on an elastic foundation or the finite element methods on both the inside and outside radii. The circumferential stresses measured experimentally on the inside radius agree well with the beam on elastic foundation solution while on the outside radius the agreement between the experimental data and the finite element solution is very good.

The comparison for the moment loading is shown in Figures 17 and 18. Agreement was excellent for the 15.0" cylinder. Agreement was good for the 7.5" cylinder as well except for the circumferential stresses on the inside where the experimental data predicted a stress less than that for beam on elastic foundation or finite elements.

The influence of the loading fixture used in Dohrmann's and Ives'

experiment was not completely damped out close to the top of the cylinder [1] This will influence agreement in all cases near where the load was applied.

### **Saint-Venant's length.**

The Saint-Venant's length divided by the length of the cylinder analyzed versus the radius to thickness ratio  $R/t$  is shown in Figures 19 and 20 in Chapter 4 for 15.0" long cylinders and for 7.5" long cylinders respectively. It is to be expected that as a cylinder gets thinner, or in other words as the radius to thickness ratio increases, the method of applying the load should have less influence on the outcome of the stress values. For all six cases the stress values will converge closer to the top of the cylinder where the load is applied for thinner cylinders than for thicker cylinders. As shown in the figures, the Saint-Venant's length does decrease as the cylinder geometry gets thinner.

### **Error.**

The percent error between the finite element solution and the beam on elastic foundation solution versus the radius to thickness ratio  $R/t$  is shown in Figures 21 and 22 in Chapter 4 for the shear loading for the 15.0" long cylinders and the 7.5" long cylinders respectively. The moment loading results are shown in Figures 23 and 24 in Chapter 4 for the 15.0" long cylinders and the 7.5" long cylinders. Using the thin cylinder formulas, equations 116-119, the plots show that the percent error, taken at the maximum stress after the Saint-Venant's length, decreases as the cylinder geometry gets thinner. Using the thick cylinder

formulas, equations 121-124, which compute the correct neutral axis and moment of inertia for the sector of a cylinder, the same general trend is shown for thinner cylinders and thicker cylinders for the moment loading, and as expected the percent error tends to be lower. However, for very thick cylinders with an edge shear load, the percent error seems to behave out of the general trend of the rest of the data. This aberration requires more investigation and was not pursued as the beam on an elastic foundation method appears to only be useful for  $R/t$  ratios higher than those in this range.

These plots may be used to determine the satisfactory use of the beam on an elastic foundation formulas. For a desired accuracy, the radius to thickness ratio may be read from the plots. For example, if a percent error of 5 is desired, the values shown in Table 2 are read from the charts. Satisfactory solutions tend to be governed on the shear loading for both 15.0" and 7.5" length cylinders since the shear loading tends to give a more conservative value of the  $R/t$  ratio than the moment loading for the same percent error. If thin cylinder formulas are

**Table 2.** Radius to thickness values for 5% error

FIGURE	DESCRIPTION	THIN OR THICK EQUATIONS	R/t
Figure 21	Shear Load on 15.0" long cylinders	Thin	13
		Thick	12
Figure 22	Shear Load on 7.5" long cylinders	Thin	13
		Thick	12
Figure 23.	Moment Load on 15.0" long cylinders	Thin	6
		Thick	2
Figure 24	Moment Load on 7.5" long cylinders	Thin	6
		Thick	2



to be used, a percent error of 5 or less may be obtained for cylinders with a radius to thickness ratio of 13 or higher for the 7.5" long cylinders and the 15 0" long cylinders. Use of the thick cylinder formulas will reduce this somewhat. A percent error of 5 or less may be obtained for cylinders with a radius to thickness ratio of 12 or higher for 7 5" and 15 0" long cylinders

### **Benefits.**

A number of benefits result from this study. It is advantageous to know the influence of the Saint-Venant's length when performing a finite element analysis. Care must be taken when examining stresses at a distance close to where the load is applied. Also, knowledge of the accuracy of the beam on an elastic foundation solution can save time by providing prior knowledge of stress levels before a detailed finite element analysis is completed. This knowledge also allows for quick estimating and speed of response in the preliminary stages of design.

### **Summary.**

The purpose of this thesis is to determine a range of ratios  $R/t$  for which a beam on an elastic foundation solution is feasible for end loadings on thick and thin cylindrical shells. Using the finite element method a Saint-Venant's length was determined for each cylindrical geometry analyzed by loading the cylinder with an end shear load in six different ways and computing the standard deviation to determine when the stress values converged along the length of the

cylinder. This procedure was repeated for the moment loading and then the two lengths were combined into one Saint-Venant's length for the cylinder geometry. Taking this Saint-Venant's length into account the maximum stress is found and the percent error computed between the finite element solution and the beam on an elastic foundation solution for each cylinder geometry. As expected the Saint-Venant's length influence decreases as the cylinder geometry became thinner. Using the plots of the percent error versus the ratio  $R/t$  a range of ratios can be found for which a beam on an elastic foundation solution is satisfactory.

Benefits result such as knowledge of the influence of the Saint-Venant's length when performing a finite element analysis, quick estimating and speed of response in the early stages of design, and prior knowledge of stress levels by use of the beam on an elastic foundation equations.

## REFERENCES

## REFERENCES

1. Dohrmann, R.J , and Ives, K D., Experimental Investigation of Edge Loading of Thick Cylindrical Shells, presented at Second SESA International Congress on Experimental Mechanics, Washington D C , September 28-October 1, 1965
2. Timoshenko, S , and Goodier, J N , Theory of Elasticity, McGraw-Hill Book Company, Inc , New York, NY, 1951, p 33
3. Hetenyi, M , Beams on Elastic Foundation, The University of Michigan Press, Ann Arbor, Mich , 1958, p 2.
4. Hetenyi, M , Beams on Elastic Foundation, The University of Michigan Press, Ann Arbor, Mich., 1958, p vi
5. Hetenyi, M , Beams on Elastic Foundation, The University of Michigan Press, Ann Arbor, Mich , 1958, pp. 30-32
6. MacGregor, C W., and Coffin, Jr , L F , Approximate Solutions for Symmetrically Loaded Thick-Walled Cylinders, J. Appl Mech , Vol 14, p A-301, 1947
7. Hetenyi, M , Beams on Elastic Foundation, The University of Michigan Press, Ann Arbor, Mich , 1958, pp 52-53
8. Hetenyi, M., Beams on Elastic Foundation, The University of Michigan Press, Ann Arbor, Mich , 1958, p 35
9. Hetenyi, M , Beams on Elastic Foundation, The University of Michigan Press, Ann Arbor, Mich , 1958, p 46
10. Porter, Michael, P.E , FEA Step by Step With Algor, Dynamic Analysis, 3415 W 93<sup>rd</sup> Street, Leawood, Kansas 66206, 1993, p 21
11. Beckwith, Buck, and Marangoni, Mechanical Measurements, 3<sup>rd</sup> Edition, Addison-Wesley Publishing Company, Reading, Massachusetts, 1982, p 277
12. Spotts, M F , Design of Machine Elements, 6<sup>th</sup> Edition, Prentice-Hall, Inc , Englewood Cliffs, N.J , 1985, p 24
13. Spiegel, Murrage, R , Schaum's Outline Series, Theory and Problems of Complex Variables, McGraw-Hill, New York, NY, 1993, p 4

- 14 Hetenyi, M., Beams on Elastic Foundation, The University of Michigan Press, Ann Arbor, Mich , 1958, pp 9
- 15 Hetenyi, M , Beams on Elastic Foundation, The University of Michigan Press, Ann Arbor, Mich , 1958, pp 3-4
- 16 Hetenyi, M., Beams on Elastic Foundation, The University of Michigan Press, Ann Arbor, Mich., 1958, pp 10-14
- 17 Hetenyi, M , Beams on Elastic Foundation, The University of Michigan Press, Ann Arbor, Mich , 1958, pp 38-43
18. Porter, Michael, P E , FEA Step by Step With Algor, Dynamic Analysis, 3415 W. 93<sup>rd</sup> Street, Leawood, Kansas 66206, 1993, p 56-57
- 19 Riddle, Douglas F., Calculus and Analytic Geometry, Wadsworth Publishing Company, Inc , Belmont, California 94002, 1979, p 66

## VITA

Sherry Caperton was born in Louisville, Kentucky on November 21, 1963. She attended school in the public system of Maury County, Tennessee where she graduated from Santa Fe High School in June, 1982. She entered Columbia State Community College, Columbia, Tennessee in the fall of 1982 where she received an Associate of Science degree in Pre-Engineering in May, 1984. In the fall of 1984 she entered Tennessee Technological University, Cookeville where in December, 1986 she received a Bachelor of Science degree in Mechanical Engineering. She entered the University of Tennessee Space Institute in the fall of 1993 to pursue a Master of Science degree in Mechanical Engineering. The Master's degree was received May, 2000.

She is presently working as an engineer at Arnold Engineering Development Center in Tullahoma, Tennessee.